Solubility characteristics of soil humic substances as a function of pH: mechanisms and biogeochemical perspectives

Xuemei Yang[1,2], Jie Zhang[1], Khan M.G. Mostofa[1,3*], Mohammad Mohinuzzaman[1,4], H. Henry Teng[1,3], Nicola Senesi[5], Giorgio S. Senesi[6], Jie Yuan[7], Yu Liu[1,3], Si-Liang Li[1,3], Xiaodong Li[1,3], Baoli Wang[1,3], and Cong-Qiang Liu[1,3*]

[1]School of Earth System Science, Tianjin University, 92 Weijin Road, Tianjin 300072, China.
[2]Institute of Ecology, College of Urban and Environmental Sciences, Peking University, Beijing, 100091, China
[3]Tianjin Key Laboratory of Earth Critical Zone Science and Sustainable Development in Bohai Rim, Tianjin University, Tianjin 300072, China
[4]Department of Environmental Science and Disaster Management, Noakhali Science and Technology University, Noakhali, Bangladesh.
[5]Dip.to di Scienze del Suolo, della Pianta e degli Alimenti, Università degli Studi di Bari "Aldo Moro", Via G. Amendola 165/A, 70126 BARI – Italy.
[6]CNR - Istituto per la Scienza e Tecnologia dei Plasmi (ISTP) - sede di Bari Via Amendola, 122/D - 70126 Bari, Italy.
[7]College of Resources and Environment, Xingtai University, Quanbei East Road 88, Qiaodong District, Xingtai City, Hebei Province.

**Corresponding author:* Khan M.G. Mostofa or Cong-Qiang Liu (mostofa@tju.edu.cn or liucongqiang@tju.edu.cn)

Abbreviations

DOC: Dissolved organic carbon
DOM: Dissolved organic matter
EEM: Excitation-emission matrix
HS: humic substances
HA: humic acids
FA: fulvic acids
PLS: protein-like substances
PLF: protein-like fluorescence
HLF: humic-like fluorescence EF: electrochemical force
IF: intramolecular force
EF_N: net EF
IF_N: net IF
LS: Labile state
CS: Complexed state
HS_{LS}: LS HS
HS_{CS}: CS HS
$HA_{LS\text{-}pH6}$: LS HA deposited at pH 6
$HA_{CS\text{-}pH6}$: CS HA deposited at pH 6
$HA_{LS\text{-}pH1}$: LS HA deposited at pH 1
$HA_{CS\text{-}pH1}$: CS HA deposited at pH 1
FA_{LS}: LS FA
PLS_{LS}: LS PLS
FA_{CS}: CS FA
PLS_{CS}: CS PLS
SOC: Soil organic carbon

SOM: Soil organic matter

Abstract

Soil humic substances (HS) typically alter their electrochemical behaviors in the pH range of 1–12, which simultaneously regulates the stability of organo-minerals by modifying the HS functionalities. This process facilitates both biotic and abiotic transformations, which consequently leads to the export of degradative byproducts (e.g. HS components, nutrients) from soils into surrounding aquatic environments through water and/or rainwater discharges. However, the solubility features, environmental consequences, and mechanisms of HS, including humic acids (HA), fulvic acids (FA), and protein-like substances (PLS), under different pHs remain unclear. To respond to these issues, we used two soil extracts which were fractionated in the pH range from 12 to 1. The pH-dependent presence or absence of fluorescence peaks in the individual HS components reflected their functional group proton/electron exchange features at both low and high pH values, which were related to their solubility or insolubility. In particular, alkaline pH (≥ pH 9) yielded the anionic forms (–O– and –COO–) of phenolic OH and carboxyl groups of HA_{CS} resulted in decreased electron/proton transfer from HS functionalities, as indicated by the decline of fluorescence peak maxima, whereas the protonic functionalities (e.g., −COOH, −OH) of HS at lower pH resulted in the formation of highly available and remains uncomplexed HS forms. The solubility of HA fractions increases with increasing pH, whereas their insolubility increases with decreasing pH, which determines their initial precipitation at pH 6 and final precipitation at pH 1, amounting approximately to 39.1-49.2% and 3.1-24.1% of the total DOM, respectively, in the two soils. Elemental anlysis results demonstrated that the C and N contents of $HA_{LS\text{-}pH6}$ were lower and those of O, S and H higher than those of $HA_{CS\text{-}pH6}$, suggesting the preservation of C and N without S acquisition in $HA_{CS\text{-}pH6}$ possibly because of their complexed with minerals, which, in turn, would determine the insolubility of the $HA_{CS\text{-}pH6}$ fraction. FA_{CS}+PLS_{CS} showed relatively higher C and S contents, and lower O% with respect to FA_{LS}+PLS_{LS}, impling that FA_{CS}+PLS_{CS} would remain under mineral protection. Fourier Transform Infrared **(**FTIR) results show significantly reduced infrared absorptions (e.g. 3300–3600 and 800-1200 cm^{-1}) of $HA_{CS\text{-}pH6}$ with respect to $HA_{LS\text{-}pH6}$, suggesting the existence of strong intermolecular interactions among HA functional groups, possibly due to insoluble forms originally complexed with minerals. But FA_{LS}+PLS_{LS} exhibited stronger bands at 3414-3429 cm^{-1} and 1008-1018 cm^{-1} than FA_{CS}+PLS_{CS}, implying a strong interaction among functional groups possibly derived from various organo-mineral complexes in FA_{CS}+PLS_{CS}. These results would indicate that HS insolubility arises via organo-metal

and organo-mineral interactions at alkaline pH, along with HApH6 insolubility via rainwater/water discharge, whereas HA_{pH2}+FA+PLS appears to be soluble at acidic pH, thereby being transported in ambient waters via rainwater/water discharge and groundwater infiltration. Therefore, the pH-dependent behaviour of soil HS greatly contributes to a better understanding of the progressive transformation, mobility/transportation, and immobility/accumulation of HS components under various environmental conditions, with relevant implications for sustainable soil management practices and soil DOM dynamics.

Key words: Paddy and maize soils; humic acids; fulvic acids; protein-like substances; acidic-alkaline pH; EEM-PARAFAC analysis; Fourier Transform Infrared

1 Introduction

Soil organic matter (SOM), especially its more chemically active components, that is humic substances (HS), are particularly important because they play a number of fundamental roles, including the control of soil fertility, climate regulation and ecosystem stability (Harden et al., 2018), plant mineral nutrition and growth (Canellas and Olivares, 2014; Schmidt et al., 2007; Trevisan et al., 2010), adsorption/desorption of trace metals and radionuclides, (Boguta et al., 2019; Bryan et al., 2012; Chou et al., 2018), and soil structural stability and porosity (Bronick and Lal, 2005; Senesi and Plaza, 2007). Loss of soil organic carbon (SOC) is due to several biotic and abiotic processes, (Crowther et al., 2016; Huang and Hall, 2017) including heterotrophic respiration (Bond-Lamberty and Thomson, 2010; Heitmann et al., 2007; Klüpfel et al., 2014; Huang and Hall, 2017) and increasing temperatures due to climate change (Davidson and Janssens, 2006). SOC loss is also affected by soil erosion caused by deforestation, tillage, and other natural degradation processes, including hillslopes, salinisation, waterlogging, and wildfires (Ellerbrock et al., 2016; Peinemann et al., 2005; Steinmuller and Chambers, 2019; De la Rosa et al., 2012; Drake et al., 2019). In general, HS are divided according to their water solubility at various pH values into humic acids (HA), which are insoluble at pH < 2; fulvic acids (FA) and protein-like substances (PLS), which are soluble under both acidic and alkaline conditions; and humin, which is insoluble at any pH (Zhang et al., 2023; Senesi and Loffredo, 1999; Mohinuzzaman et al., 2020).

Three-dimensional (3D) fluorescence excitation-emission matrix (EEM) spectroscopy (3D EEMS) is a precise, rapid and relatively simple technique for measuring filtered environmental surface waters and samples extracted from soils and sediments (Senesi, 1990a; Coble, 1990, 1996; Stedmon et al., 2003; Mostofa et al., 2013; Mohinuzzman et al., 2020). In particular, this technique allows the characterization of fluorescent components, including soil HS, autochthonous humic-like substances, PLS, detergent-like substances, and others, without the need for further pretreatment of the samples (Senesi, 1990a; Coble, 1990, 1996; Stedmon et al., 2003; Mostofa et al., 2013). Recently, 3D EEM combined with parallel factor (PARAFAC) analysis has been used to identify and characterise HA, FA, and PLS (Stedmon et al., 2003; Gao et al., 2018b; Tadini et al., 2020; Mohinuzzaman et al., 2020). In particular, two typical protein-like fluorescence (PLF) peaks (T and T_{UV}) and a minor component consisting of one or two fluorescence peaks (M and/or A) attributable to humic-like fluorescence (HLF) were identified in PLS (Mohinuzzaman et al., 2020; Yang et al., 2024).

The HS solubility and insolubility mechanisms are associated with two key factors. First, the soil pH, which varies widely in soils worldwide (Table S1), influences the ionisation level of HS functional groups. In particular, high pH values favour anionic forms, i.e., $-COO^-$ and $-O^-$ of carboxylic acids and phenolic/alcoholic groups and, consequently, the formation of metal-HS complexes, including insoluble ones (Brady and Weil, 2008; Kleber et al., 2007; Min et al., 2014; Dynarski et al., 2020; Kirsten et al., 2021; Zhang et al., 2023). In contrast, relatively low soil pH values favour protonic forms, such as, –COOH and –OH of HS functionalities, which promote proton/electron exchange processes (Klapper et al., 2002; Nurmi and Tratnyek, 2002; Cory and McKnight, 2005; Yang et al., 2016; Wang et al., 2023). Furthermore, the zeta potential (ZP) of HA is minimal in the pH range 5–7, which is most likely caused by the

dissociation of acidic functional groups that prevail at lower pH values, whereas disaggregation predominates over dissociation at higher pH values (Jovanović et al., 2013). Second, significant variability in the pH of rainwater (Table S2) or any inflowing water can affect both the solubility/transport/mobility and insolubility/immobilization/accumulation of soil HS. Thus, understanding the solubility/insolubility of SOM/HS under changing pH conditions is important for understanding the global C cycle.

Earlier studies (Hemingway et al., 2019; Lützow et al., 2006; Marschner et al., 2008; Sollins et al., 1996; Vogel et al., 2014) have not paid much attention to these issues when assessing the solubility and insolubility of SOM/HS. For example, pH effects were studied to assess the interaction mechanisms of Fe(II) ions with soil HA at pH values of 5 and 7 (Boguta et al., 2019), the binding of Cu and Pb to HA and FA at pH 4-8 (Christl et al., 2005), Cu(II) binding properties of soil FA at pH 7.0 (dos Santos et al., 2020), coagulation mechanisms of HA in metal ion solutions at pH 4.6-7.0 (Ai et al., 2020), coagulation behaviours of HA in Na^{+} and Mg^{2+}solutions at pH 3.6, 7.1, and 10.0 (Wang et al., 2013), and the disaggregation kinetics of peat HA at pH 3.65-5.56 (Avena and Wilkinson, 2002), but not directly in water and alkali-extracted soil HA, FA and PLS fractions. The acidic and alkaline pH conditions in the soil liquid phase alter the electronic configuration of the functional groups of HS components, which in turn affect their complexation capacity (Christl et al., 2005; Zhang et al., 2023; Avena and Wilkinson, 2002). The solubility and insolubility mechanisms of the HS components under different pH conditions remain unknown. In particular, two key fundamental questions regarding the effects of pH on HS are still unclear, that is, how the electrochemical behaviour of soil HS components changes in the pH range of 1–12, and how these changes affect the solubility/insolubility features of HS components and their mobilization/immobilization during rainwater runoff and groundwater infiltration in soil.

Although the soil pH varies from 2.80 to 9.39 (Table S1), we fractionated the extracted solution in the pH range from 12 to 1 for several key reasons: Firstly, HS-bound as organo-minerals primarily liberate HS components and other constituents (e.g., various metals) in the liquid phase under alkaline extraction (0.1 M NaOH ≈ pH 13.0). Thus, it is crucial to understand how these HS components change their properties from pH 12 to 1. Secondly, it is essential to investigate how HS, in particular HA-bound DOC, due to its insoluble nature behave within the pH range from 12 to 1.

Most importantly, the solubility of HS components and their subsequent mineralization are very relevant factor for the availability of soil nutrients and trace elements and the activity of soil microorganisms, while their stability in organo-minerals affects negatively these processes (Malik et al., 2018; Varghese et al., 2024; Lange et al., 1998; Gao et al., 2025; Soti et al., 2015; Yang et al., 2024; Gilbert et al., 2007; Zhang et al., 2023). These issues are concurrently associated with the corresponding biological fixation/sequestration of C, N and S by soil photosynthetic microorganisms (Green et al., 2019; Varghese et al., 2024; Heckman et al., 2001; Levicán et al., 2008; Ma et al., 2021; Kelly et al., 2021; Gao et al., 2025), and the subsequent release of extracellular polymeric substances and/or HS components in the neoformation of fresh organo-minerals in soil (Whalen et al., 2024; Yu et al., 2020; Paul, 2016; Kallenbach et al., 2016).

Therefore, Therefore, the solubility or insolubility of soil HS components is crucial for a better understanding of both soil management and soil carbon dynamics.

Therefore, the main objective of this study was to ascertain the solubility characteristics of soil HS components under different pH conditions (pH 1–12) by analysing their fluorescence properties following extraction from two different soils using either water or an alkaline solution. Water-extractable HS are designated labile-state (LS) HS and are mostly subject to runoff from surface water and leaching from groundwater (Mohinuzzaman et al., 2020; Gao et al., 2018a). Alkali-extractable HS are designated as complexed-state (CS) HS and typically occur as organo-mineral and organo-metal complexes in soils (Kirsten et al., 2021; Lalonde et al., 2012; Hemingway et al., 2019; Kleber et al., 2021). Furthermore, to assess the electrochemical behaviour of soil HS components and their molecular-level characteristics based on their pH-dependent solubility, we also analysed $HA_{LS/CS}$ precipitated at pH 6 ($HA_{LS/CS\text{-}pH6}$) and pH 1 ($HA_{LS/CS\text{-}pH1}$) and a mixture of FA and PLS (FA_{LS}+PLS_{LS} and FA_{CS}+PLS_{CS}) at pH 1. Another key objective of this work was to provide a comprehensive view of the solubility and insolubility of soil HS based on the mechanisms involved in the electronic configurational changes of HS reactive acidic functional groups, i.e., either in the protonic forms (e.g., −COOH, −OH) or in the anionic forms (e.g., $-COO^-$, $-O^-$) under various pH conditions. This will provide a better understanding of soil properties and processes for sustainable agricultural management.

2 Materials and methods

2.1 Soil samples

Soil samples were taken from two locations in China: a maize field and rice paddy field (Fig. S1). The maize field soil is classified as calcaric fluvisol (WRB et al., 2015) and is located near the Beijing–Tianjin highway, approximately 20 km from the city of Tianjin. The rice paddy soil is classified as fluvi-stagnic luvisol (WRB et al., 2015) and is located near Shanghai. The two soils were cultivated for approximately 50 and 30 years, respectively. Importantly, the rationale for selecting paddy and maize soils is based on their distinct characteristics, i.e., paddy soils are submerged for extended periods, while maize soils are relatively less influenced by the presence of water. Therefore, HS components of these two soil types are expected to be altered very differently in their organo-mineral lability and stability in the pH range from 1 to 12. This study is expected to provide useful information on soil carbon dynamics and contribute to minimize soil carbon loss during agricultural practices. At each site, three soil subsamples were randomly collected from the top horizon A (0–30 cm) and mixed homogeneously to produce a spatially representative sample at the field scale. After oven drying to constant weight at 40°C, the samples were passed through a 2-mm sieve. Table S3 provides information on the sampling sites, vegetation cover, and major physicochemical characteristics of the two soil types.

The soil particle size was measured using the hydrometer method with a Mastersizer 3000 (Malvern, Table S3). The soil extracts (see below) were obtained from 0.2-mm-sieved soils after mortar grinding with a pestle.

2.2 Protocol used to extract water and alkali soluble SOM/HS

In the first part of the experiment, the soil liquid phase was extracted from the two soils using either water or an alkaline solution (0.1 M NaOH), which operationally represent, respectively, the water-extractable labile state (LS) and the water insoluble alkali-extractable complexed state (CS) of SOM/HS (Mohinuzzaman et al., 2020). The detailed extraction procedure is shown in the flow diagram in Fig. S2. Briefly, the water extracts were obtained using ultrapure water (18.2 MΩ·cm, Mill-Q, Millipore) with a soil/water ratio of 1:10. The mixtures were vortexed for 1 min in closed 500-ml brown bottles before being shaken for 24 h in an orbital shaker (200 revs per min) at 25°C. The mixtures were then centrifuged for 20 min at 4000 rpm (Thermo Fisher Scientific). SORVALL ST 16) for removing suspended solids. The supernatant solutions were then filtered through a 0.45-µm glass-fibre filter (GF/F type, Shanghai Xin Ya Purification Equipment Co. Ltd, China) to remove any remaining particulate matter. The solutions were then frozen at –20°C.

To obtain the alkaline extracts, the suspended soil residues from water extraction were sequentially extracted under N_2 with a 0.1M NaOH solution at a soil residue/alkaline solution ratio of 1:10 (Fig. S2). In this case, the mixtures were also vortexed for 1 min, shaken at 200 rpm for 3 h at 25°C, and then centrifuged for 20 min at 4000 rpm using the same centrifuge as before to remove suspended solids. The supernatant solutions were then filtered through a 0.45-µm membrane filter (polytetrafluoroethylene membrane, PTFE**,** Shanghai Xin Ya Purification Equipment Co. Ltd, China) to remove any remaining particulate matter. Under alkaline conditions, PTFE filters are highly effective at separating solutions from particulate matter (Mohinuzzaman et al., 2020). The remaining solid residue was extracted with a fresh alkaline solution for 3 h, and the above procedure was repeated. The supernatant solutions were then mixed with former solutions and frozen at −20°C for further processing. The original pH values for the water-extracted paddy and maize samples were 8.13 and 7.92, respectively, while alkali-extracted samples were 13.02 and 12.98, respectively.

2.3 Protocol used to isolate solid HA and FA+PLS samples by acidification of water and alkaline extracts

The second part of the experiment involved two distinct approaches. To adjust the pH from 12 to 1, aliquots of 45 mL of water or alkaline extracts were placed in 50-mL glass bottles, and then the pH was progressively adjusted to certain value in the range 12 to 1 by adding 0.1 and 1 mol L^{-1} NaOH or HCl solutions with a 10-µL chromatographic sampler (minimum scale 0.2 µL). As the maximum amount of acid/base reagent added to each sample was < 1.0 mL, the dilution effect could be ignored. A Thermo Orion water quality tester, calibrated before each measurement, was used to determine the pH of the solutions prior to further analytical measurements. Three replicates (n = 3) were used for each pH adjustment experiment. All experiments were performed under laboratory ambient temperature of 25°C.

In the other approach, approximately 400 mL of water extracts or alkaline extracts were placed in individual 500-mL glass bottles, the pH was adjusted to 6 using HCl (0.1 and 1 mol L^{-1}) and left for 10 h at 25°C to allow the precipitation of HA_{LS} and HA_{CS}, respectively (Fig. S2). The precipitates, denoted as HA_{LS} at pH 6 ($HA_{LS\text{-}pH6}$) and HA_{CS} at pH 6 ($HA_{CS\text{-}pH6}$) were separated by centrifugation (Thermo Fisher Scientific, SORVALL ST 16) at 3000 rpm for 5 min. The supernatants were then adjusted to pH 1 using the same procedure described above, yielding HA_{LS} ($HA_{LS\text{-}pH1}$) and HA_{CS} ($HA_{CS\text{-}pH1}$). The remaining supernatants at pH 1 were classified as FA_{LS}+PLS_{LS} and FA_{CS}+PLS_{CS} mixtures. The HA precipitates and FA + PLS solutions were freeze-dried before further analysis.

2.4 Analytical methods

The elemental compositions of the HA isolated at pH 6 and 1 and the freeze-dried mixture of FA + PLS were measured using an elemental analyser (Elemental Vario E.L. III, Germany). Approximately 20 mg of each dried, ground, and homogenised sample was placed in a clean, carbon-free, pre-combusted tin boat placed on an autosampler rack assembly and loaded onto the elemental analyser. Sulfanilamide was used as the standard after every ten measurements. The O content was calculated by difference formula: O% = 100-C%-H%-N%-S%.

Fluorescence (excitation-emision matrix, EEM) spectra were obtained using a fluorescence spectrophotometre (F-7000, Hitachi, Japan), as previously described (Mohinuzzaman et al., 2020; Yang et al., 2021). To ensure instrument performance and data quality every ten samples were measured with ultrapure (18.2 MΩ.cm) water as a blank. The water EEM spectra were subtracted from the sample EEM spectra. A 4-μg L^{-1} quinine sulfate (QS) solution in 0.01 N H_2SO_4 was used for fluorescence normalisation. The fluorescence intensities of each sample were calibrated using the intensity of the QS (1 μg L^{-1} = 1 QS unit, QSU) peak at Ex/Em = 350/450 nm (Mohinuzzaman et al., 2020). To avoid inner-filter effects and fluorescence quenching, the extracted solutions were diluted prior to EEM measurements based on the initially measured DOC concentration (Tadini et al., 2018). The fluorescence intensity of each peak was rechecked and corrected using the absorbance-based method proposed by Kothawala et al. (Kothawala et al., 2013).

The pre-processed EEM data were then subjected to PARAFAC analysis using the N-way Toolbox for MATLAB, (Andersson and Bro, 2000) as previously described **(**Stedmon et al., 2003**)**. First, the Rayleigh and Raman peaks and the ultrapure water blank spectrum were subtracted from each experimental EEM spectrum using a homemade Excel program (Mohinuzzaman et al., 2020). To avoid mixing the fluorescent components of different soil samples, which could produce artefacts (Mostofa et al., 2019), PARAFAC analysis was performed individually for each selective samples. Finally, nonnegative constraints were applied to the PARAFAC model. The detailed procedure used for PARAFAC analysis of the EEM spectra has been described previously (Mohinuzzaman et al., 2020).

The Fourier Transform Infrared (FTIR) spectra were recorded on 2 mg aliquots of each dehydrated HA isolated at pH 6 and 1, as well as each freeze-dried mixture of FA + PLS, which were mixed with 200 mg of

dried KBr, and pelletised by pressing under reduced pressure. The spectra were measured over the range of 4000–400 cm^{-1} by averaging 30 scans at a 4-cm^{-1} resolution using an IR Affinity-1S spectrometer (Shimadzu, Japan) that included a high-energy ceramic light source, a temperature-controlled, high-sensitivity DLATGS detector, and a high-throughput optical element, which allowed the optimisation of the electrical and optical systems to achieve the highest signal-to-noise (SN) ratio.

3 Results and discussion

3.1 Fluorescence spectra

The fluorescence peaks of HA, FA, and PLS in the EEM spectra of the water and alkaline extracts of each sample (original and adjusted pH) were identified individually by applying the PARAFAC model (Figs. 1, 2; Table 1). The fluorescence properties of the original samples were similar to those measured in an earlier study (Mohinuzzaman et al., 2020), but the EEM images and fluorescence peaks of all three components (HA, FA, and PLS) identified in the pH-adjusted samples exhibited distinct differences. Such differences could be attributed to the pH-influenced changes in protonation/deprotonation of the each component's functional groups, which could either suppress or favour electron transfer processes from the functional groups to the solution (Mostofa et al., 2013; Senesi, 1990b). Two fluorescence peaks were identified in the HA (peaks C and A) and FA (peaks M and A) components, while four peaks were identified in the PLS fraction: peaks M and A for HLF, and peaks T and T_{UV} for PLF (Mohinuzzaman et al., 2020).

3.1.1 Characteristics of $HA_{LS\text{-}pH6/pH1}$ and solubility of HA_{CS}

The EEM-PARAFAC model detected no fluorescence in water-extracted HA_{LS} at acidic pH ranging from 6 to 1 (Fig. 1). This causes HA to precipitate at pH 6 ($HA_{LS\text{-}pH6}$) and at pH 1 ($HA_{LS\text{-}pH1}$), accounting for approximately 48.3-49.2% and 3.1-10.8% of total DOC_{LS}, respectively based on initial DOC_{LS} concentrations of 13.4 and 24.5 mg/L, respectively in paddy and maize soils (Fig. 3). Absence of fluorescence or precipitation at pH < 7 suggests that HA_{LS} may naturally stabilise in soil during rainfall/water runoff at pH values ≤ 6 due to its water insolubility. However, at higher pH levels, the fluorescence peak maxima (C: 310-340/432-460 and A: 250-275/432-460) and intensities varied significantly (Fig. 1 and 3; Table 1). The highest C and A peak intensities of HA_{LS} were observed at pH 7, with a gradual decrease as pH increased in both soil HA_{LS}. At pH 7-8 (peaks C: 325-340/432-440 nm and A: 275/432–440 nm; Table 1), the functional groups can donate their electrons, thus increasing their fluorescence intensity, whereas the blue shift and decreasing intensity of the fluorescence peaks with increasing pH are caused by the deprotonation/ionization of COOH and OH functional groups. The deprotonated functional groups would form organo-metal complexes through donation of π–electron to *d*-orbitals of metal ions particularly Fe ions, (Zhang et al., 2023) which insolubilise HS/SOC in soil (Kirsten et al., 2021; Six et al., 2002; Lalonde et al., 2012; Hemingway et al., 2019; Kleber et al., 2021; Makiel et al., 2022). In contrast, the red-shift of the fluorescence peaks could be attributed to easier electron transfer from the functional groups of HA (Mostofa et al., 2013; Senesi, 1990b).

Unlike HA_{LS}, the excitation/emission peaks of HA_{CS} at pH 1-10 in maize soil were detected at wavelengths (C, 345-385/460-477 and A, 275-280/460-477 nm) that were longer than those of the corresponding HA_{LS} at pH 7-10 (C, 325-345/432-477 and A, 260-280/432-477 nm) (Fig. 2, Table 1). These results would suggest that HA at pH 2 may be the insoluble form of HS bound to various minerals/metals, (Kirsten et al., 2021; Curtin et al., 2011; Lalonde et al., 2012; Hemingway et al., 2019) whereas the longer wavelength peaks (C and A) of alkali-extractable HA_{CS} functionality remains mineral protection (Mohinuzzaman et al., 2020). The two peak maxima at longer wavelengths (350/486 nm and 275/486 nm at pH 7-8 in HA_{CS} from paddy soil and at 380/477 nm and 275/477 nm at pH 3-4 in HA_{CS} from maize soil might be ascribed to electron transfer from thiol- and/or N-containing functional groups and/or highly aromatic ring structures in alkaline-extracted HA (Fulda et al., 2013; Haitzer et al., 2002, 2003; Szulczewski et al., 2001), as well as to binding sites reacting with metal ions (Wu et al., 2004a, b). These groups are significantly affected by environmental factors and soil conditions (Jiang et al., 2015; Vidali et al., 2010). In particular, an increase in acidity might shift peak C of soil HA_{CS} from a shorter to a longer excitation wavelength but does not affect peak A detected at pH 3-4 (C, 360-380/466-477 nm and A, 270-275/466-477 nm) and pH 5-6 (C, 340-345/469-477 nm and A, 270-275/469-477 nm) (Fig. 2; Table 1). These results would imply that increasing the acidity promotes electron transfer from the peak C-type functional groups of HA_{CS}.

The shorter emission maxima of peaks C and A in HA_{CS} at pH 11-12, i.e., 458 and 458 nm, and 426 and 426,460 nm, respectively, for paddy and maize soils (Table 1), would suggest that electrons released from HA_{CS} functional groups were primarily suppressed by extreme alkalinity conditions, as they would require higher energy, as confirmed by the appearance of peaks of decreased intensity at shorter wavelengths (Fig. 3). Thus, HA showed a higher electron transfer capacity in paddy soils than in maize soils (Xi et al., 2018).

Furthermore, the significant decrease in the two peak intensities in HA_{CS} at pH 1–6 would be primarily due to precipitation at pH 6 and pH 1, which amounted approximately to 39.1-46.4% and 3.1-24.1%, respectively, of the initial DOC_{CS} concentrations of 35.2 and 79.4 mg/L, respectively, in paddy and maize soils (Fig. 3). The higher peak intensities at pH 1-2 than at pH 3-4 (Fig. 4) would suggest that some functional groups were labile at this pH, thus favouring electron transfer from HA_{CS} in both soils; this was also confirmed by the longer wavelength of the excitation/emission peak C at pH 1-2.

3.1.2 Behavior of FA_{LS} and FA_{CS} as a function of pH

Both FA_{LS} and FA_{CS} showed higher intensities of the two peak maxima at pH 3-4, (i.e., 325-335/439-460 and 270/439–460 nm, respectively) and at pH 1-4, (i.e., 315-340/449-460 and 260-270/449–460 nm, respectively) than at alkaline pH, with the former showing a blue shift with respect to the latter for both soils (Figs. 1, 2; Table 1). The pH-dependent differences arising in FA_{LS} might be due to existing environmental factors (e.g. moisture, temperature/climatic warming, redox properties, mineral matrix, agricultural practices, vegetation, and microbial activities), whereas those in FA_{CS} might remain under mineral protection because of their occurrence in organo-mineral complexes (Kirsten et al., 2021; Mohinuzzaman et al., 2020; Lehmann and Kleber, 2015; Gao et al., 2018a). Moreover, peak M disappeared at pH 7–8 and a minor peak appeared

in the original FA_{LS}, suggesting degradation of the functional groups in FA_{LS} at pH 7–8. The longer-wavelength peak maxima measured at extremely acidic pH 1–4 would indicate easier electron/proton transfer from the protonated phenolic groups in both FA_{LS} and FA_{CS} (Klapper et al., 2002; Nurmi and Tratnyek, 2002; Cory and McKnight, 2005; Yang et al., 2016; Wang et al., 2023). In contrast, increasing the pH would imply the ionisation of phenolic groups, which would necessitate more energy for the electron transfer process, resulting in peak maxima at shorter wavelengths under alkaline conditions.

The wavelength differences detected for peak maxima were accompanied by differences in their intensity, which was the highest for peak M of FA_{LS} at pH 6 and increased by approximately 362% and 20.0%, respectively, in paddy and maize soil FA_{LS}, compared with the original FA_{LS}. This indicates that protonated functional groups can transfer electron more easily than deprotonated functional groups. In contrast to FA_{LS}, the highest peak M intensity of FA_{CS} from paddy soil occurred at pH 12 and gradually decreased to pH 5, whereas FA_{CS} from maize soil showed the highest intensity at pH 3 and decreased up to pH 9 (Fig. 4), suggesting a difference in peak M functional groups between the two soils. These features may be ascribed to the different environmental conditions in the two soils, that is, long-term submersion in paddy soil and a drier state in maize soil (Mohinuzzaman et al., 2020).

Peak A intensity followed a similar trend for both soils, peaking at pH 10 and 8, then gradually decreasing to pH 5–6 by 57% for the paddy soil and pH 3–4 by 41% for the maize soils (Fig. 4). These results suggest that peak A functional groups in the FA_{CS} of the two soils behave similarly. The highest peak intensity of FA_{CS} in the two soils was detected at pH 3; but these peaks were absent in FA_{LS} (Figs. 1 and 2). These results suggest the presence of new functional groups in FA_{CS} that are absent in water-soluble FA_{LS}. The decreasing intensity of peak A toward either extremely acidic (pH 1-2) or alkaline (pH 11-12) conditions suggests an increased suppression of electron release at either very high or very low pH conditions. Notably, both FA_{LS} and FA_{CS} exhibited the highest solubility under acidic conditions, such as pH 3 and pH 6, respectively.

3.1.3 Behavior of PLS as a function of pH

Peak M of HLF in the PLS_{LS} from maize soil was most prominent at acidic pH, with very low intensity at pH 7–8, and disappearing entirely at pH 9–12 (Figs. 1, 4). These results might be ascribed to the easy electron transfer from the corresponding functional groups under acidic conditions and to the suppression of electron release under alkaline conditions. However, this peak was completely absent in the PLS_{LS} from the paddy soil at any pH condition, possibly due to the long-term favoured hydrolysis occurring under submerged conditions, which does not occur in the drier maize soil where this fraction is not degraded (Mohinuzzaman et al., 2020).

The PLS_{LS} samples from both soils exhibited two PLF peaks, that is, T and T_{UV}, at pH 7-8, with peak T (245/303 nm) that completely disappeared at acidic pH 1-6, but was dominant at pH 9-12. This may imply a marked influence of the pH on the ionisation of the functional groups. In contrast, the PLS_{CS} from the paddy soil showed PLF peaks (T and T_{UV}) in the pH range of 3 to 10, whereas in the PLS_{CS} from maize soil, they were predominant at acidic pH 1-6, appeared as minor peaks at alkaline pH 7-10 and disappeared at pH 11-

12 (Fig. 2, Table 1). Notably, $PLS_{CS,}$ like $FA_{LS/CS}$, might undergo rapid electron/proton exchange reactions that result in the appearance of predominant peak maxima under acidic conditions, whereas the disappearance of PLF peaks at pH 11-12 might arise, similar to $FA_{LS/CS}$, from the anionic forms of PLS, which might be involved in stable organo-mineral complexes. In this case, the submerged conditions existing in the paddy soil are primarily responsible for the predominant occurrence of PLF peaks in the PLS_{CS}, whereas the drier conditions of maize soil (high temperature and low precipitation) cause extensive degradation of the PLF components, with the predominant presence of the HLF components. However, the significant increase in the peak intensities of both HLF and PLF in PLS_{CS} at pH 6 implies that the responsible functional groups would remain in a protonated state (Fig. 4), which suggests a marked pH effect on the functional groups of PLS_{CS}. Similar pH-influenced changes in the peak T_{UV} intensities have been reported for extracellular polymeric substances (Zhang et al., 2010).

Finally, the predominant presence of PLF and HLF components in PLS_{CS} compared to PLS_{LS} suggests their origin from newly formed insoluble complexes with minerals/metals (Ciceri and Allanore, 2015; Curtin et al., 2011; Mohinuzzaman et al., 2020; Song et al., 2016). Furthermore, the presence of a PLF peak at 240-245/303-305 nm at pH 9-12 in PLS_{LS}, which was not detected in PLS_{CS}, supports its origin in PLS degradation under environmental conditions. The dominant presence of the HLF peaks in both PLS_{LS} and PLS_{CS} may facilitate electron transfer from the corresponding functional groups, which is a key factor in their solubility under acidic conditions.

3.2 Soil properties and elemental composition of HS

The soil total carbon (STC) and soil organic carbon (SOC) in the paddy soil (14.22 and 10.82 mg/g, respectively) were higher than in the maize soil (13.13 and 8.76 mg/g, respectively), whereas the soil total nitrogen (STN) in maize soil (0.78 mg/g) was higher than that of paddy soil (Table 1 in Mohinuzzaman et al., 2020). The clay and silt contents were significantly higher in the maize soil (8.6% and 57.6%, respectively) than in the paddy soil (2.5% and 38.3%, respectively), whereas the sand content in the paddy soil (36.0%) was higher than that in the maize soil.

The C and N contents of $HA_{LS\text{-}pH6}$ from both soils were lower than those of O, S, and H, and all atomic ratios were higher than those of $HA_{CS\text{-}pH6}$ (Table 2). These results would suggest the preservation of C and N without S acquisition in $HA_{CS\text{-}pH6}$ possibly because of their complex state with minerals (Hemingway et al., 2019; Marschner et al., 2008; Vogel et al., 2014), which, in turn, determines the insolubility of the $HA_{CS\text{-}pH6}$ fraction. In contrast, the lower levels of C and N and the high content of S that characterise $HA_{LS\text{-}pH6}$ would suggest the degradation of the N-containing functional groups (Mohinuzzaman et al., 2020; Li and Vaughan, 2018; Senesi and Loffredo, 1999) and the acquisition of S-containing compounds, possibly from soil fungi (Masaki et al., 2016; Saito et al., 2002; Whelan and Rhew, 2015), which, in turn, would determine the solubility of the $HA_{LS\text{-}pH6}$ fraction.

Due to the lack of sample $HA_{LS\text{-}pH1}$ from maize soil, no comparison was possible with the corresponding $HA_{CS\text{-}pH1}$. However, $HA_{CS\text{-}pH1}$ from paddy soil showed extremely low C%, N%, and atomic ratios and very

high O%, H%, and S% compared to the corresponding $HA_{LS\text{-}pH1}$, indicating its insolubility at pH 1, that is, this HA fraction would remain under mineral protection in soil (Hemingway et al., 2019; Marschner et al., 2008; Vogel et al., 2014). It is possible that the decrease in C and increase in O in the $HA_{CS\text{-}pH1}$ fraction in paddy soil were affected by high water availability and microbial respiration (Fang et al., 2005; Huang and Hall, 2017; Yu et al., 2020; Chen et al., 2020).

The main features of all the FA+PLS samples were their very low C, N, C/S, C/H, and C/O ratios and very high O%, H%, and S% with respect to the corresponding HA fractions discussed above (Table 2). In particular, FA_{CS}+PLS_{CS} showed relatively higher C and S contents and C/H and C/O ratios, and lower O% with respect to FA_{LS}+PLS_{LS}, which would suggest that, similar to HA_{CS} samples, FA_{CS}+PLS_{CS} would remain under mineral protection in the soil. The higher S content of FA_{LS}+PLS_{LS} from paddy soil than that of maize soil might be ascribed to the uptake and conversion of carbonyl sulfide (COS), possibly operated by soil fungi or microorganisms in the paddy soil (Li et al., 2010; Masaki et al., 2016; Saito et al., 2002; Whelan and Rhew, 2015), whereas S would be rapidly degraded by biotic and abiotic processes in the drier maize soil (Liu et al., 2007; Masaki et al., 2016; Whelan and Rhew, 2015). Similarly, the relatively lower C% in FA_{LS}+PLS_{LS} and FA_{CS}+PLS_{CS} from paddy soil compared with maize soil might be ascribed to extended oxidative degradation and/or hydrolysis processes occurring in paddy soil, which lead to extended mineralisation processes (Fang et al., 2005; Huang and Hall, 2017; Yu et al., 2020; Chen et al., 2020). Finally, the high O% in the FA + PLS samples might have contributed to the presence of O-rich PLS extracted together with FA.

3.3 Fourier Transform Infrared (FTIR) spectra

The FTIR spectra of all tested samples (Fig. 5; Table 3) were typical of soil HS (Senesi and Loffredo, 1999), but they exhibited a number of different characteristics. First, $HA_{CS\text{-}pH6}$ had significantly lower IR absorptions than $HA_{LS\text{-}pH6}$ in both soils, particularly in the range 3300–3600 and 800–1200 cm^{-1}. This suggests strong intermolecular interactions among HA functional groups, possibly due to insoluble forms complexed with minerals/metals (Gabor et al., 2015; Mostofa et al., 2018). This has an impact on the overall bonding system in the conjugated macromolecular HA structure. Furthermore, these insoluble forms require relatively high energy for electron transfer, resulting in a decrease in the relative intensity of all bands in $HA_{CS\text{-}pH6}$ compared to $HA_{LS\text{-}pH6}$. Second, the band at 3421–3429 cm^{-1} is stronger for $HA_{LS\text{-}pH1}$ than for $HA_{LS\text{-}pH6,}$ indicating the presence of more free NH or OH functional groups (Demyan et al., 2012; Kunlanit et al., 2014; Senesi et al., 2003). Third, the weak band at 1015–1030 cm^{-1} (possibly attributed to S=O and C–O–S stretching of S-containing functional groups) in $HA_{LS\text{-}pH1}$ of the paddy soil and its absence in maize soil (Demyan et al., 2012; Singh et al., 2011; Shammi et al. 2017; Senesi et al., 2003), might be due to the degradative nature of $HA_{LS\text{-}pH1}$ compared to $HA_{LS\text{-}pH6}$. $HA_{LS\text{-}pH1}$ degradation is primarily caused by the degradation of its functional groups in the presence of existing environmental factors (Xie et al., 2004; Mohinuzzaman et al., 2020; Lehmann and Kleber, 2015). Fourth, the samples FA_{LS}+PLS_{LS} generally exhibited stronger bands at 3414-3429 cm^{-1} and 1008-1018 cm^{-1} than FA_{CS}+PLS_{CS} (Gabor et al., 2015; Kunlanit et al., 2014; Mostofa et al.,

2018), which suggested a strong interaction among functional groups possibly generated from various silicates/mineral complexes in FA_{CS}+PLS_{CS}, whereas a weak interaction would have yielded free functional groups in LS samples featuring strong bands by loosely bound electrons in functional groups. Fifth, the presence of two relatively intense bands at 3711–3745 and 3838–3873 cm^{-1} in all HA samples could be attributed to aromatic C-H stretching in individual aromatic ring structures, while aromatic C-H in conjugated systems absorb at 3080–3030 cm^{-1} (Kunlanit et al., 2014; Demyan et al., 2012; Senesi et al., 2003).

3.4 Mechanisms determining the insolubility/solubility of HA and FA+PLS

Two molecular parameters, the electrochemical force (EF), also known as the intermolecular force, and the intramolecular force (IF), are thought to control the mechanisms underlying the solubility/insolubility of HA and FA + PLS (Fig. 6). In particular, EF includes intermolecular van der Waals forces, London forces, dipole-dipole and ion-dipole interactions, and hydrogen bonds between molecules, whereas IF refers to the intramolecular forces between bonded atoms in a molecule (Aeschbacher et al., 2010). In particular, the decrease in the net EF (EF_N) could be attributed to the protonation of the functional groups in HA, which decreases their electron-donating capacity in aqueous solutions (Ai et al., 2020; Chassapis et al., 2010; Ritchie and Michael Perdue, 2003). In contrast, an increase in net IF (IF_N) can be attributed to increase intramolecular interactions between various functional groups via hydrogen bonding in HA (Ai et al., 2020; Benes, 2009; Boguta et al., 2019; Noy et al., 1997; Vezenov et al., 2005, 1997). Strong competition exists between EF_N and IF_N; when $IF_N > EF_N$ under acidic conditions, all functional groups associate, resulting in HA precipitation from the solution.

The solubility of $FA_{LS/CS}$ + $PLS_{LS/CS}$ at all acidic pH values was related to their higher total acidity, which resulted from a higher number of elemental oxygen atoms (Table 2) which belong to oxygenated functional groups and have a relatively lower molecular size than HA (Leenheer et al., 1995; Robarge, 2018). These features would cause a relatively low IF_N value and a relatively high EF_N value owing to the formation of external H-bonding with the solution components. This interpretation was supported by the presence of two peaks for each FA and an HLF peak in the PLS at pH 1–4 (Figs. 2 and 4; Table 1). These results would confirm the easier electron transfer from the functional groups to the solution at acidic pH, resulting in $EF_N > IF_N$ implying their dissolution at extremely acidic pH (Fig. 6).

3.5 Solubility/insolubility characteristics of soil HS and their environmental consequences

The solubility/insolubility of the HS components was influenced by each specific pH unit, with the involvement of various functional groups (Fig. 6) (Avena and Wilkinson, 2002; Boguta et al., 2019, 2016; Garcia-Mina, 2006; Hernández et al., 2006) which might occur through various processes such as complexation, ion exchange, adsorption, aggregation/coagulation, and flocculation (Avena and Wilkinson, 2002; Lippold et al., 2007; Wang et al., 2013; Jovanovic et al, 2013). In particular, (a) $HA_{CS\text{-}pH6}$/$HA_{LS\text{-}pH6}$ and $HA_{CS\text{-}pH1}$/$HA_{LS\text{-}pH1}$ would remain in suspension under acidic conditions, whereas IF interactions preferentially

increase with increasing acidity owing to the enhanced occurrence of protonic forms of their functional groups; and (b) the disappearance of fluorescence peaks (C, M, A, T, or T_{UV}) of specific functional groups of individual HS components under any pH condition in solution would cause their interactions either with other functional groups or coagulation/precipitation with metals or minerals (Chen et al., 2014; Helms et al., 2013; Zhang et al., 2023; Hemingway et al., 2019; Lützow et al., 2006; Marschner et al., 2008; Sollins et al., 1996; Vogel et al., 2014). Furthermore, each individual pH unit may sterically affect the HS functional groups (Boguta et al., 2019; Senesi, 1990a, 1990b), which would result in either the appearance or disappearance of a fluorescence peak and/or a change in the fluorescence intensity of specific peaks (Figs. 2, 3, 4, Table 1). These effects may be associated with an increase or decrease in the electron donation capacity of the fluorescent functional groups in HS (Cory and McKnight, 2005; Senesi, 1990a; Klapper et al., 2002; Karadirek et al., 2016; Wang et al., 2023), thus determining their solubility/insolubility.

An overall conceptual model of the possible processes and mechanisms is outlined in Fig. 6 and summarised below.

(1) The deprotonated state of the functional groups (e.g. $–COO^-$) in HA_{LS} constantly donates electrons to various soil components, thus activating a series of biogeochemical processes. Rainwater (usually at $pH \leq 6$) or water discharge/runoff cannot dissolve HA_{LS} and, partly, HA_{CS}. Particularly, $HA_{LS/CS\text{-}pH6}$ that would be insoluble/not mobile in soil during rainwater events and water runoff at $pH \leq 6$, suggesting natural protection during transport along the soil profile and in ambient surface waters. In contrast, $HA_{LS/CS\text{-}pH1}$ is mobile and transported to ambient surface waters via rainwater, leaching, and groundwater infiltration (Ronchi et al., 2013; Stolpe et al., 2013; Mostofa et al., 2019).

(2) Under acidic conditions, down to pH 1, the functional groups of $HA_{CS/LS\text{-}pH1}$ remained protonated, thus reducing electron transfer capacity. This feature of $HA_{CS/LS\text{-}pH1}$ might explain some recent results, e.g. the decline of metal binding capacity of HS at low pH (Christl et al., 2005), the low effect of HA on plant growth (Asli and Neumann, 2010; Mora et al., 2012), the decline of HA capacity in binding organic pollutants (Jones and Tiller, 1999; Tremblay et al., 2005), and the decrease in carbon mineralisation at low pH with a fivefold decrease in bacterial growth and a fivefold increase in fungal growth (Rousk et al., 2009).

(3) Higher pH increases deprotonation of functional groups (e.g. $–COO^-$) of $HA_{LS/CS}$ allowing for easier electron transfer to soil components like minerals and fungi (Chen et al., 2020; Yu et al., 2020), increasing the solubility of metal ions (Firestone et al., 1983; Flis et al., 1993), e.g. from metal sulfides (Chou et al., 2018), soil respiration and carbon mineralization (Pietikäinen et al., 2005; Rousk et al., 2009), and degradation of –COOH/–OH upon exposure to UV-Vis light (Spence and Kelleher, 2016; Ward et al., 2013; Xie et al., 2004).

(4) The predominant presence of two $FA_{LS/CS}$ peaks at pH 1-2, which were absent at neutral or alkaline pH (Figs. 2 and 4), suggests the solubility of these HS components under acidic conditions. In turn, this condition affects the capacity for complexation/decomplexation and/or sorption/desorption of metal ions and organic pollutants, thus modifying their mobility/transport by rainwater/water discharge/runoff and groundwater leaching (Tadini et al., 2020; Mostofa et al., 2019) and their distribution, toxicity, and bioavailability in soil

(Anastasiou et al., 2014; dos Santos et al., 2020; Tadini et al., 2020; Zhu and Ryan, 2016). In particular, the $FA_{LS/CS}$ fractions in acidic conditions easily leached down the soil profile via rainwater discharge, as occurs in the podsolization process (Lundström et al., 2000).

(5) The predominance of HLF in PLS_{LS} and PLF in PLS_{CS} at acidic pH (Figs. 2 and 4) may be primarily responsible for their high solubility under acidic conditions, which implies high mobility and easy transport in ambient water environments and groundwater leaching (Gao et al., 2018a; Mohinuzzaman et al., 2020).

(6) The knowledge of the molecular-level solubility of the three HS components is essential for a better understanding and management of agricultural practices, as affected by their individual solubility, tendency to precipitate, and variable capability to form organo-minerals, which can occur more or less rapidly/slowly (Underwood et al., 2024; Zhang et al., 2023). For instance, the HA fractions of acidic soils may either partially precipitate or remain in suspension due to an increase in IF_N from increasing intramolecular interactions among various functional groups via hydrogen bonding, influenced by acidic conditions as discussed earlier. As a result, precipitated HA fractions would enhance C stability, while suspended HA fractions are highly prone to leaching by rainwater runoff. Furthermore, the high solubility of FA and PLS under acidic conditions would result from prolonged water saturation occurring in paddy fields, which will lead to soil C loss by their transport due to rainwater runoff. Simultaneously, these conditions of HS are expected to contribute to increase the salinity levels in such type of soils (Varghese et al., 2024; Ma et al., 2021). Therefore, high-water-demand crops such as rice may not be suitable for maintaining C stability in acidic soils. In contrast, low-water-demanding crops like maize and wheat would be more effective in minimizing C loss from acidic soils. On the other hand, alkaline soils can support the cultivation of a wide variety of crops while minimizing C loss, along with the presence of relatively high levels of HS-bound to organo-minerals. In particular, the pH levels of the paddy and maize soils object of this study are slightly alkaline (8.13 and 7.92, respectively), making them reasonably suitable for diverse types of crops. Furthermore, both soils exhibit relatively high levels of HS-bound organo-minerals, with significant increases in DOC_{CS} stability (2.6 and 3.2 times higher, respectively) compared to DOC_{LS} lability.

(7) The strategies for addressing pH-affected soil carbon loss primarily involve the significant loss of dissolved HS, particularly fulvic acids and protein-like fractions, from acidic soils due to water and rainwater runoff. Therefore, it is crucial to implement an efficient, rapid and sustainable drainage system that operates on a relatively short time scale, so that HS components may become less likely to dissolve in water and rainwater. Effective and timely drainage from the soil surface can help prevent carbon loss from acidic soils. Finally, the HS/SOM appeared to undergo progressive transformation under various environmental conditions (Mohinuzzaman et al., 2020), yielding various forms of HS components (Figs. 2 and 4). Furthermore, pH appears to control the chemical nature and electronic configuration of HA/FA/PLS functional groups, influencing their solubility/insolubility and consequently their mobilization/immobilization and transport/accumulation, thereby markedly affecting all biogeochemical functions and processes in the soil. The features and extension of such processes would depend mostly on the existing environmental conditions and factors, such as pH, soil type, organisms (e.g. bacteria, fungi, and

552 vegetation), temperature variations due to climate change, and precipitation frequency and intensity
553 (Mohinuzzaman et al., 2020; Pietikäinen et al., 2005; Rousk et al., 2009).

554 **4. Conclusions**

555 The presence, absence, or variable relative intensity of the fluorescence peaks of HS components under
556 different pH conditions and their relationship with electron release from their functional groups appeared to
557 be an excellent indicator of the HS component status. In particular, an alkaline or elevated pH level would
558 result in anionic forms ($–O^-$ and $–COO^-$) of phenolic OH and carboxyl groups of HA, FA and PLS, which
559 ultimately contributes to the insolubilisation and stability of HS through the formation of organo-mineral
560 complexes in soils. In contrast, at acidic pH, the electron and proton transfer processes would be facilitated
561 by the availability of uncomplexed metal ions, with subsequent insolubility of $HA_{LS+CS\text{-}pH6}$ which would
562 remain insoluble in soils during rainwater events or water runoff at pH 6, whereas $HA_{LS+CS\text{-}pH1}$ would remain
563 soluble and thus mobile and would be transported in ambient surface waters via rainwater, leaching, and
564 groundwater infiltration (Ronchi et al., 2013; Stolpe et al., 2013; Mostofa et al., 2019).
565 The highly soluble FA and PLS at acidic conditions would facilitate to an easy transport to ambient surface
566 waters via rainwater and groundwater discharge (Ronchi et al., 2013; Stolpe et al., 2013; Mostofa et al.,
567 2019). Furthermore, the predominant presence of PLF peaks in PLS_{CS} from pH 5 to 10 in paddy soil is
568 indicative of solubility, whereas the relatively high degradability of PLS_{LS} and PLS_{CS} in maize soil may be
569 attributed to the dry conditions (Mohinuzzaman et al., 2020).
570 Finally, the insolubility of individual HS components would arise when $IF_N > EF_N$, which would be related
571 to the formation of hydrogen bonds between the HS functional groups and the aqueous phase, whereas the
572 solubility of HS components would occur when $EF_N > IF_N$. Future research directions should focus on
573 investigating acidic soils, which are beyond the scope of this study. These soils are expected to be
574 significantly affected by the individual conditions of HA, FA, and PLS in acidic environments. In conclusion,
575 pH was confirmed to be a very important factor in determining the solubility-insolubility of HA, FA, and
576 PLS in soil and should be considered with the aim of preserving soil organic carbon.
577

Acknowledgement of funding sources

This work was financially supported by the Natural Science Foundation of China (grant numbers: 42293262**,** 41925002, U1612441 and 42230509) and by the Key Construction Program of the National "985" Project, Tianjin University, China.

Competing interests

The authors declare no competing financial interest.

Data availability

The data collected and/or analyzed during the current study are provided in the main manuscript and supplementary materials.

Author contribution

K.M.G.M. and C.Q.L. designed, conceived and supervised the project; X.Y. performed the main experiments, analysed all data and prepared all Figures. J.Z. partly performed the extraction of humic acids (HA) and fulvic acids (FA) + protein-like substances (PLS) samples from soil solution and analyzes the elemental analyses and FTIR, M.M. performed the soil sampling and their preprocessing, J.Y. and X.Y. conducted the EEM-PARAFAC analysis. K.M.G.M, N.S. and X.Y. wrote the manuscript; H.H.T. and G.S.S. reviewed and edited the manuscript. All authors discussed the data and revised the manuscript.

Table 1: Excitation/emission (Ex/Em) wavelengths (nm) of fluorescence peaks of HA, FA and PLS identified by PARAFAC analysis applied individually to EEM spectra of original water and alkaline extracts from paddy and maize soils and of their pH-adjusted solutions at pH 1-2, pH 3-4, pH 5-6, pH 7-8, pH 9-10 and pH 11-12.

Samples	Soil	Fluorescence peak (Ex/Em, nm)							
		HA		FA		PLS			
		Peak C	Peak A	Peak M	Peak A	Peak M	Peak A	Peak T	Peak Tuv
Water extracts									
Original(pH 8.13)	paddy	330/467	270/467	315/439	230/439	280/409	220/409	280/335	220/335
Original(pH= 7.92)	maize	345/477	280/477	310/440	245/440	280/404	220/404	280/339	220/339
pH 1-2	paddy	nd	nd	315/419	235/419	nd	nd	nd	nd
"	maize	nd	nd	330/442	270/442	305/417	230/417	nd-	230/308
pH 3-4	paddy	nd	nd	325/439	270/439	nd	220/416	nd	220/305
"	maize	nd-	nd	335/460	270/460	305/422	230/422	nd-	230/304
pH 5-6	paddy	nd-	nd-	310/442	265/442	nd	220/417	nd	220/303
"	maize	nd	nd	325/458	265/458	305/417	230/417	nd	230/305
pH 7-8	paddy	340/440	275/440	nd	235/431	nd	nd-	275/322	220/322
"	maize	325/432	275/432	nd	240/423	285/416	220/416	nd	220/305
pH 9-10	paddy	310/440	250/440	280/415	220/415	nd-	nd-	nd	245/305
"	maize	325/442	260/442	305/411	230/411	nd	nd	nd	245/303
pH 11-12	paddy	325/449	255/449	305/399	225/399	nd	nd	nd	240/305
"	maize	325/460	260/460	300/416	230/416	nd-	nd-	nd	245/303
NaOH extracts									
Original(pH=13.02)	paddy	335/460	260/460	320/389	240/389	275/387	225/387	nd	225/304
Original(pH=12.98)	maize	365/460	275/460	335/451	245/451	310/405	235/405	nd-	225/304
pH 1-2	paddy	nd-	nd-	315/449	260/449	310/398	225/398	nd	225/307
"	maize	-nd	nd-	340/460	270/460	310/416	225/416	nd	225/304
pH 3-4	paddy	360/466	270/466	325/440	235/440	310/369	220/369	-nd	220/307
"	maize	380/477	275/477	330/440	240/440	270/386	220/386	nd-	220/305
pH 5-6	paddy	340/469	270/469	315/403	230/403	nd-	nd	270/337	220/337
"	maize	345/477	275/477	325/440	240/440	310/399	230/399	nd-	230/311
pH 7-8	paddy	350/486	275/486	300/440	245/440	-nd	220/399	270/339	220/339
"	maize	360/460	280/460	325/440	240/440	275/421	220/421	nd-	220/310
pH 9-10	paddy	330/477	270/477	315/405	235/405	-nd	220/414	275/334	220/334
"	maize	385/460	275/460	330/440	240/440	270/404	220/404	nd-	220/305
pH 11-12	paddy	330/458	265/458	320/388	240/388	275/387	225/387	nd-	225/303
"	maize	375/426	275/426,460	335/431	245/431	nd	220/399	nd	220/308

nd: not detected

Table 2: Elemental composition (%, moisture and ash free) and atomic ratios of $HA_{LS\text{-}pH6}$, $HA_{LS\text{-}pH1}$, $HA_{CS\text{-}pH6}$, $HA_{CS\text{-}pH1}$, FA_{LS}+PLS_{LS} at pH 1 and FA_{CS}+PLS_{CS} at pH 1.

Sample	Soil	Ash content (%)	Elemental composition (%)					C/N	C/S	C/H	C/O
			C	O	H	N	C/H				
$HA_{LS\text{-}PH6}$	Paddy	0.01	56.7	37.1	2.0	3.9	0.2	17	987	2.4	2
$HA_{LS\text{-}PH6}$	Maize	0.02	54.6	39.6	2.1	3.3	0.3	19	434	2.2	1.8
$HA_{CS\text{-}pH6}$	Paddy	0.21	61.2	32.6	1.7	4.0	0.1	18	1256	3.0	2.5
$HA_{CS\text{-}pH6}$	Maize	0.41	58.7	33.3	1.5	5.6	0.1	12	1557	3.2	2.4
$HA_{LS\text{-}pH1}$	Paddy	0.13	57.0	36.8	2.0	3.8	0.1	18	1081	2.4	2.1
$HA_{LS\text{-}pH1}$	Maize	nd	nd	nd	nd	nd	nd	nd	nd	nd	nd
$HA_{CS\text{-}pH1}$	Paddy	0.08	33.8	58.1	4.5	2.9	0.5	14	165	0.6	0.8
$HA_{CS\text{-}pH1}$	Maize	0.07	61.6	32.6	1.3	4.2	0.2	17	904	4.1	2.5
FA_{LS}+PLS_{LS} at pH 1	Paddy	nd	35.2	56.8	4.8	2.2	0.8	19	124	0.6	0.8
FA_{LS}+PLS_{LS} at pH 1	Maize	0.76	37.3	53.1	5.0	2.8	0.3	15	350	0.6	0.9
FA_{CS}+PLS_{CS} at pH 1	Paddy	0.03	37.7	55.1	3.6	2.7	0.8	16	128	0.9	0.9
FA_{CS}+$PLSc_{S}$ at pH 1	Maize	0.19	44.8	48.6	3.6	1.9	0.9	27	128	1.0	1.2

nd: not detected due to lack of sample

Table 3: Major FTIR absorption bands and assignments for $HA_{CS\text{-}pH6}$, $HA_{CS\text{-}pH1}$, $HA_{LS\text{-}pH6}$, $HA_{LS\text{-}pH1}$, FA_{LS}+PLS_{LS} at pH 1 and FA_{CS}+PLS_{CS} at pH 1 for paddy and maize soils**.**

Wave number (cm^{-1})	Assignment	$HA_{LS\text{-}pH6}$	$HA_{CS\text{-}pH6}$	$HA_{LS\text{-}pH1}$	$HA_{CS\text{-}pH1}$	FA+PLS_{LS}	FA+$PLSC_{CS}$
3800-3750 3710-3680	O-H stretching, -OH (free)	strong	weak	strong	weak	weak	strong
3520-3500	O-H stretching, -OH (association), N–H stretching (trace), hydrogen-bonded OH	strong	weak	strong	weak	strong	weak
2930-2900	Aliphatic C-H stretching	weak	weak	weak	strong	weak	weak
2400-2200	Nitrile C≡N	strong	weak	strong	strong	strong	weak
1660-1630	C=O stretching of amide groups(amide I band) C=O of quinone and/or H-bonded conjugated ketones	nd	nd	nd	nd	nd	nd-
1600-1550	Aromatic C=C stretching, COO— symmetric stretching	strong	strong	strong	strong	strong	strong
1540-1510	N-H deformation and C-n stretching (amide Il band), aromatic C-C stretching	nd	nd	nd	nd	nd	nd
1420-1410	C=N stretching of primaryamides (amide Ill band)	nd	nd	nd	nd	nd	nd
1375-1275	O–H deformation and C–O stretching of phenolic OH, COO— antisymmetric stretching	weak	weak	strong	strong	strong	weak
1170-1120	C-OH stretching of aliphatic O-H	nd	nd	nd	nd	nd	nd
1020-1000	C-O stretching of polysaccharides or polysaccharide-like substances, Si-O of silicate impurities	strong	weak	strong	strong	strong	weak
880-780	Out-of-plane bending of aromatic C-H	strong	weak	strong	strong	strong	weak
500-450	In-of-plane bending of aromatic C-H	weak	strong	strong	weak	weak	weak

nd: not detected

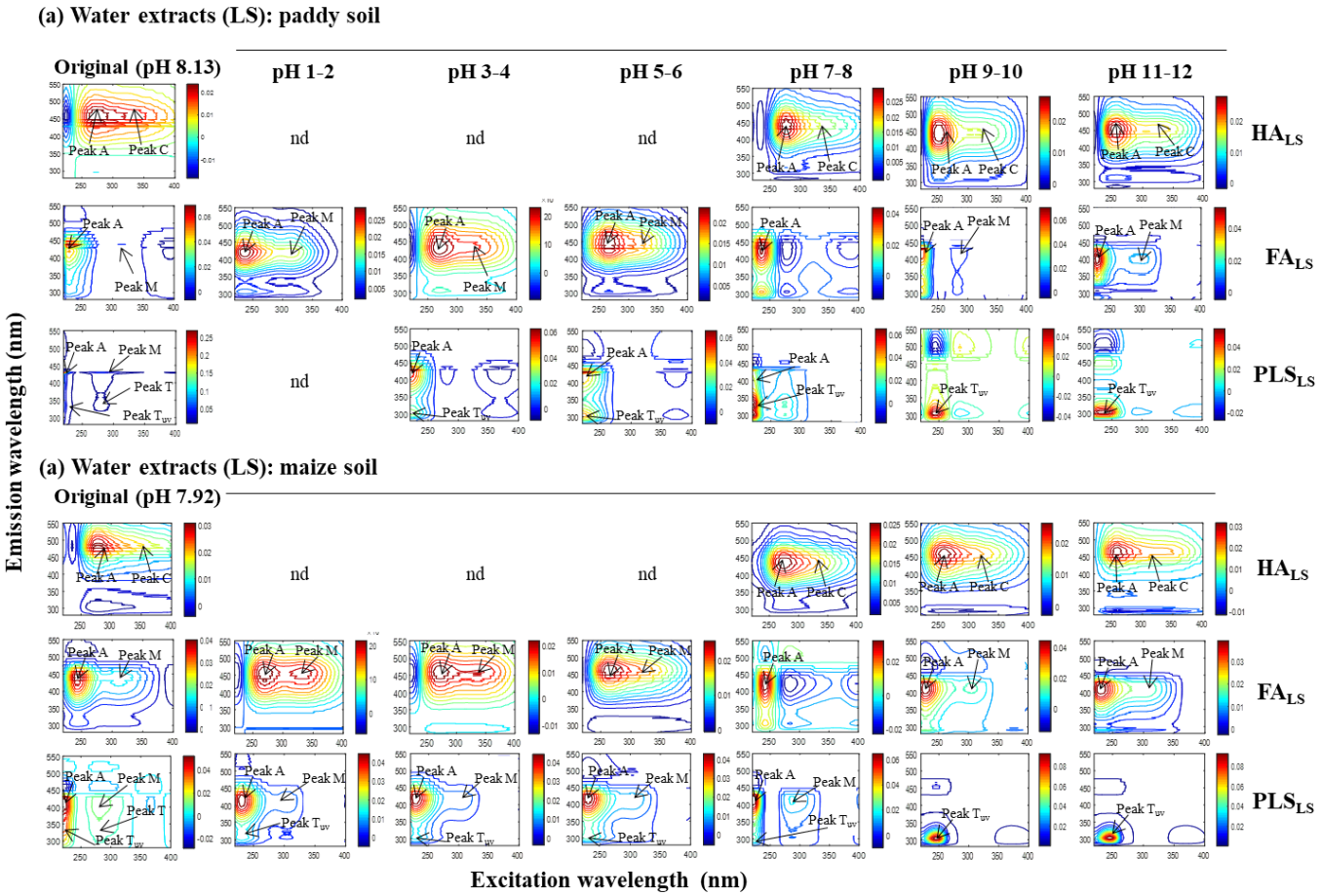

Figure 1: Fluorescence spectra and peaks identified using EEM-PARAFAC modeling in the original solution before pH adjustment and water extracts from paddy and maize soils adjusted at various pH. Water-extractable humic acid (HA) is completely precipitated in both paddy and maize soils, as evidenced by a substantial decrease in dissolved organic carbon (DOC) concentrations of 48.3% and 49.2% at pH 6, respectively. Consequently, it results not detected (nd) by the EEM-PARAFAC model. Similarly, 'not detected' for protein-like substances (PLS) in paddy soil may be due to its highly degradative nature, as its minor peaks are detected in the original solution at pH 8.13, whereas the correspondingly functionalities disappear at highly acidic pH 1-2.

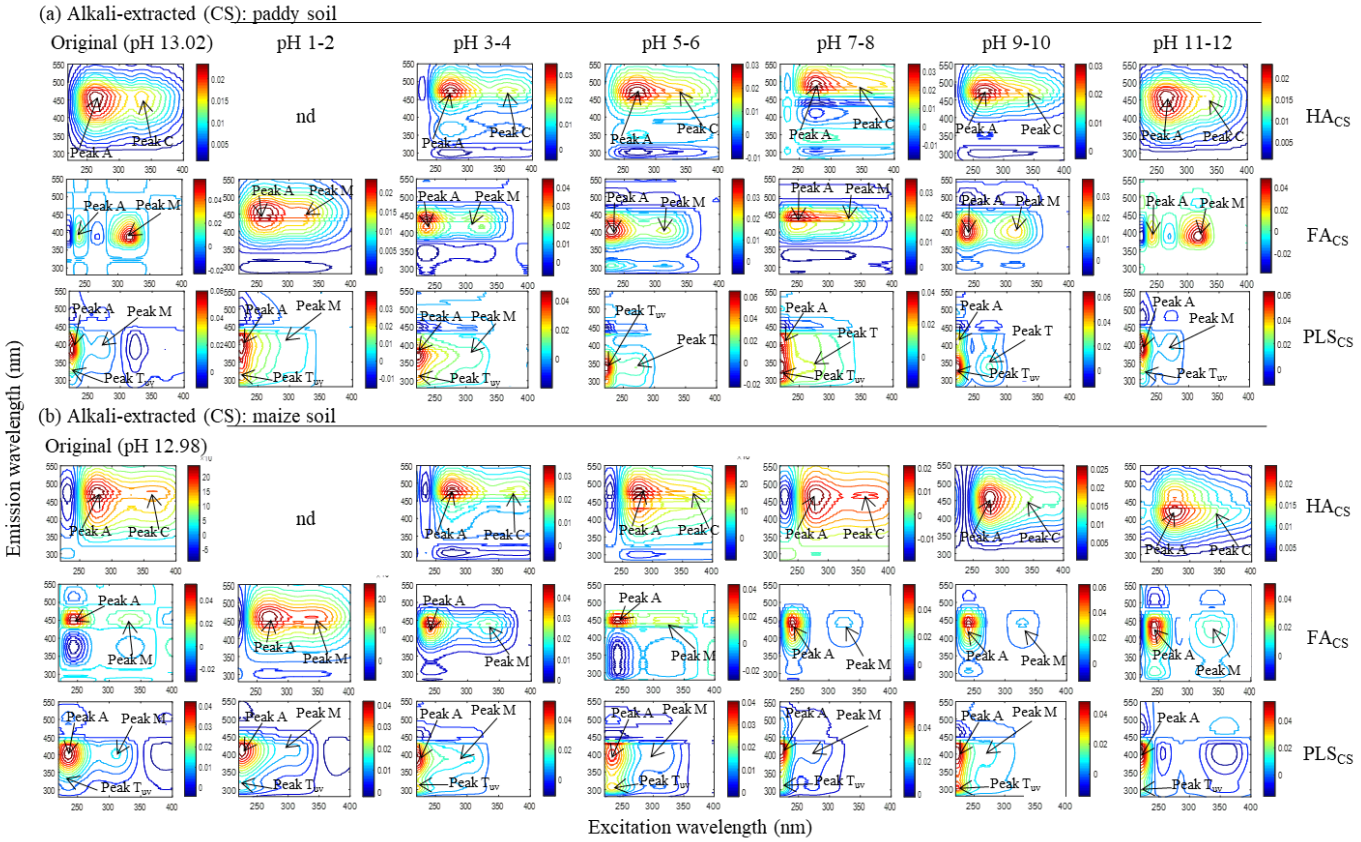

Figure 2: Fluorescence spectra and peaks identified using EEM-PARAFAC modeling in the original solution before pH adjustment and alkaline extracts from paddy and maize soils adjusted at various pH. Alkali-extractable HA is completely precipitated at pH 1 in both paddy and maize soils, which is a well-known phenomenon in soil, also evidenced by a corresponding decrease of 48.1% and 53.8% of DOC concentration at pH 1, with respect to their extracted original solutions (pH ~13). Consequently, HA at pH 1-2 result 'not detected' by the EEM-PARAFAC model. Noteworthy, the detection of alkali-extractable HA at pH levels 3-6, in contrast to its absence in water-extractable HA, may result from a significantly higher release of HA from organo-minerals, which is evidenced by the DOC in alkali-extractable HA that is 2.6 to 3.2 times greater than that in water-extractable HA. In particular, water-extractable HA is highly degradative in nature and shows relatively low concentrations, which correspondingly result in its precipitation at pH 6.

650

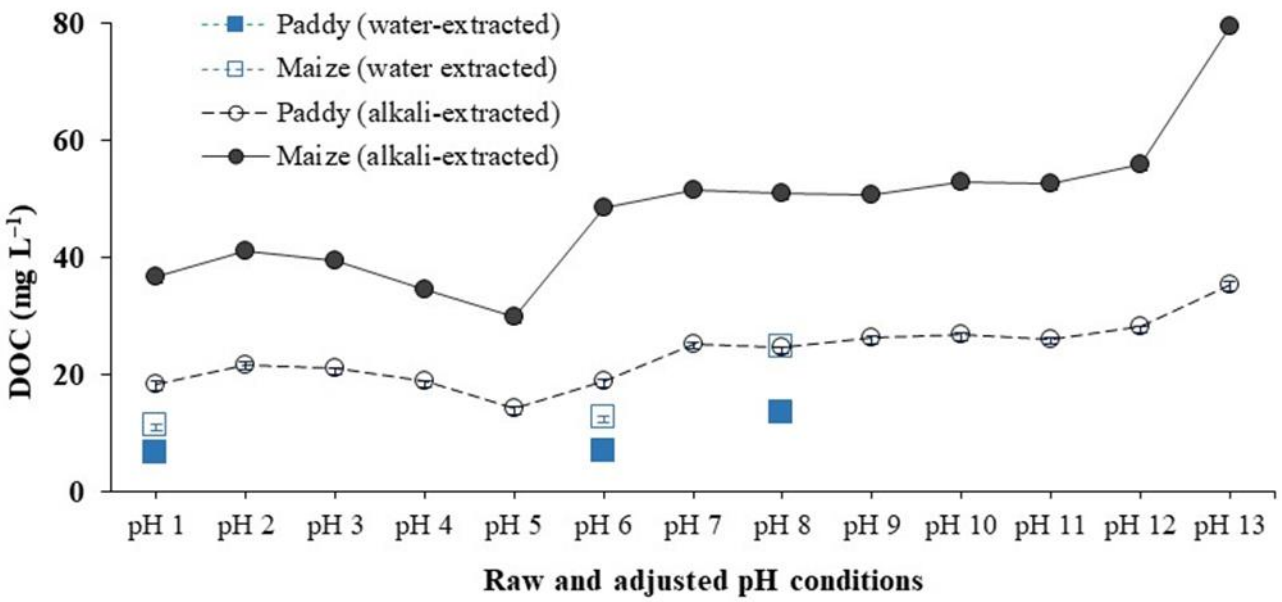

655

Figure 3. Variation in DOC concetrations of the pH-adjusted HS_{LS} and HS_{CS} from paddy and maize soils.

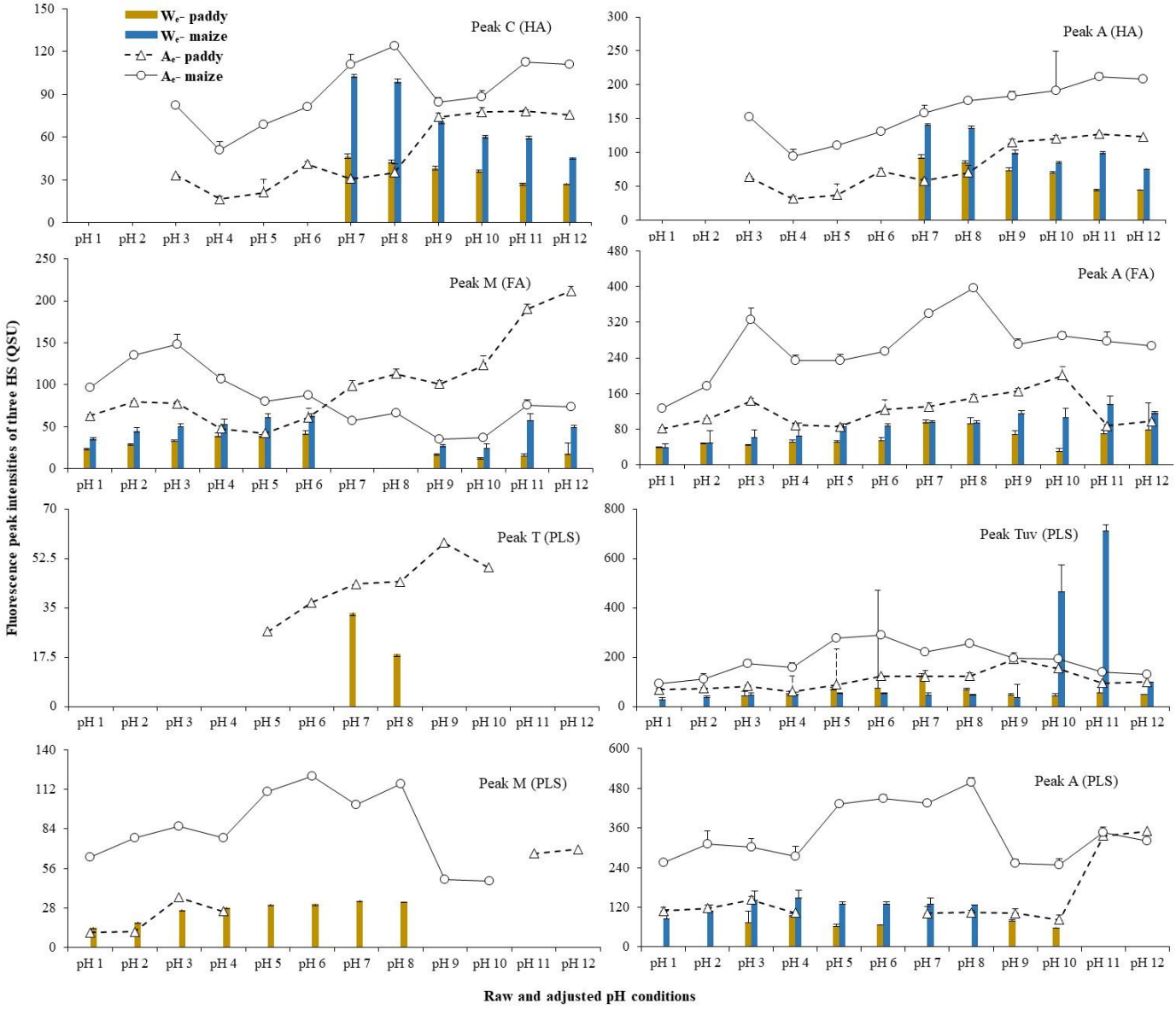

660 **Figure 4:** Fluorescence intensities of HA (peak C and peak A), FA (peak M and peak A) and PLS (peak T, peak T_{UV}, peak M and peak A) in pH-adjusted solutions of HS_{LS} and HS_{CS} from paddy and maize soils.

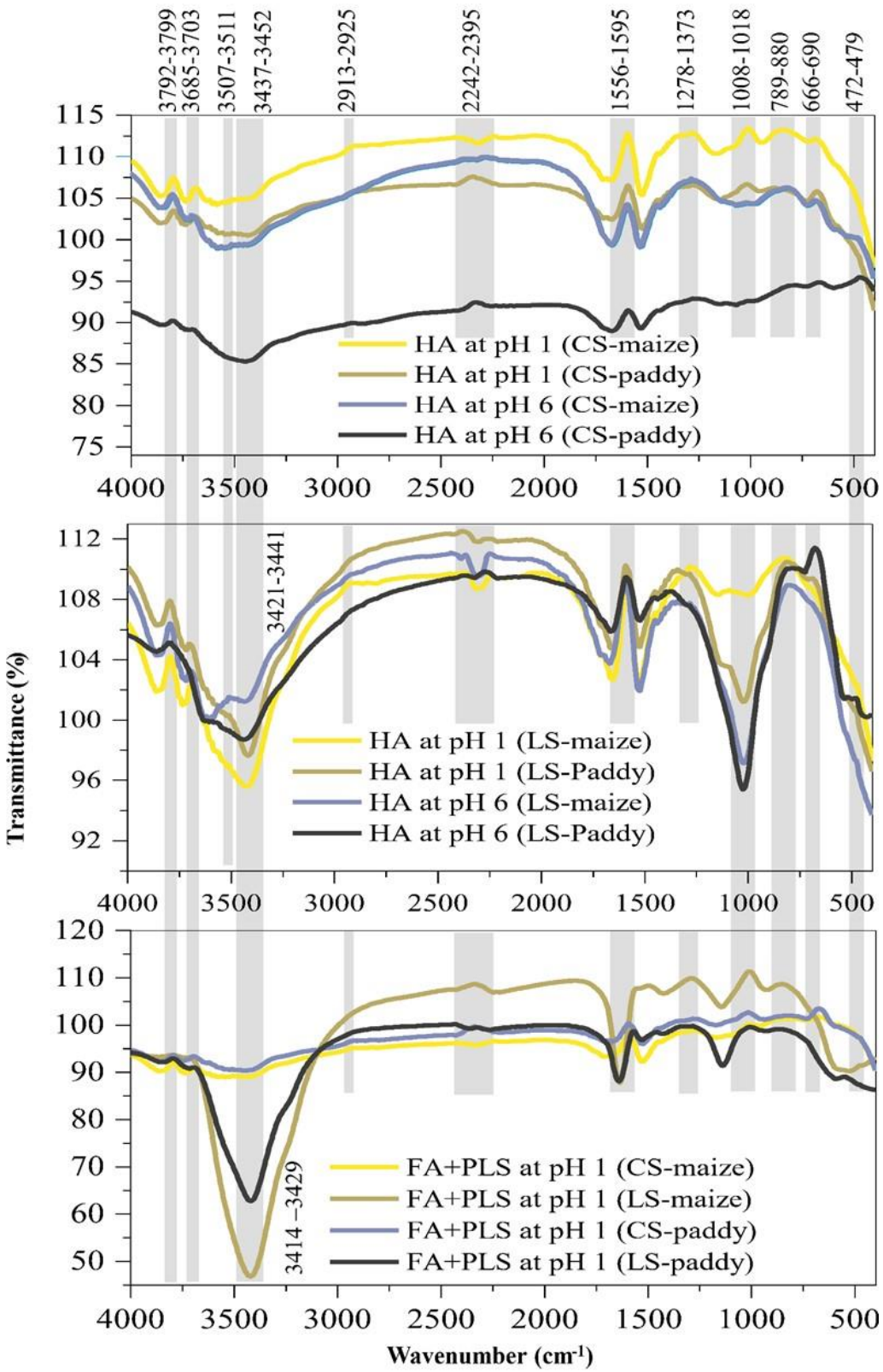

Figure 5: FTIR spectra of $HA_{LS\text{-}pH6}$, $HA_{LS\text{-}pH1}$, $HA_{CS\text{-}pH6}$, $HA_{CS\text{-}pH1}$, FA_{LS}+PLS_{LS} at pH 1 and FA_{CS}+PLS_{CS} at pH 1.

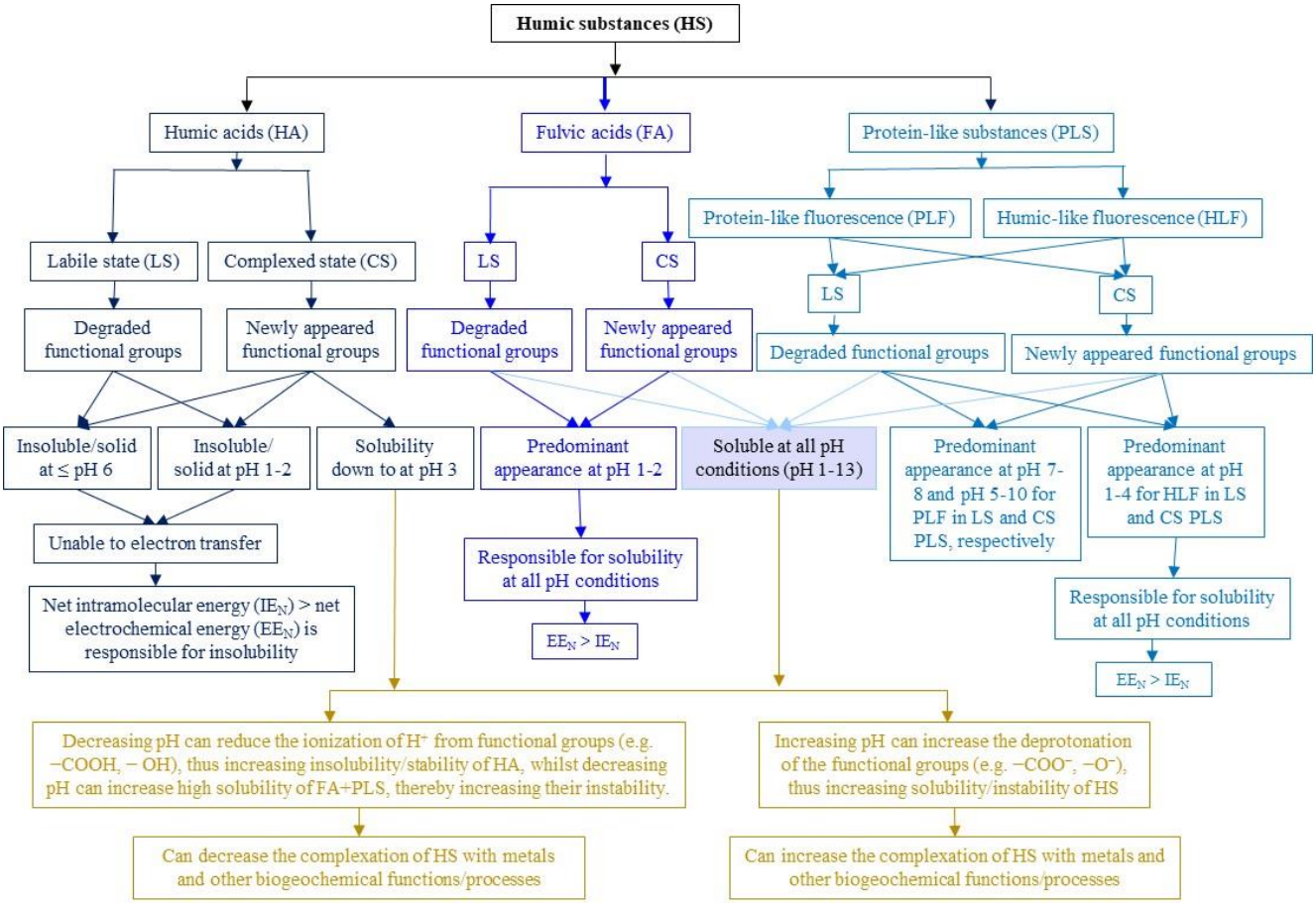

Figure 6: Conceptual model developed referring to HS_{LS} and HS_{CS}, including HA, FA and PLS, based on the presence or absence of the corresponding fluorescence peaks in different pH conditions.

References

Aeschbacher, M., Sander, M., and Schwarzenbach, R. P.: Novel electrochemical approach to assess the redox properties of humic substances, Environ Sci Technol, 44, 87–93, https://doi.org/10.1021/es902627p, 2010.

Ai, Y., Zhao, C., Sun, L., Wang, X., and Liang, L.: Coagulation mechanisms of humic acid in metal ions solution under different pH conditions: A molecular dynamics simulation, Science of the Total Environment, 702, 135072, https://doi.org/10.1016/j.scitotenv.2019.135072, 2020.

Anastasiou, E., Lorentz, K. O., Stein, G. J., and Mitchell, P. D.: Prehistoric schistosomiasis parasite found in the Middle East, Lancet Infect Dis, 14, 553–554, https://doi.org/10.1016/S1473-3099(14)70794-7, 2014.

Andersson, C. A. and Bro, R.: The N-way Toolbox for MATLAB, Chemometrics and Intelligent Laboratory Systems, 52, 1–4, https://doi.org/10.1016/S0169-7439(00)00071-X, 2000.

Asli, S. and Neumann, P. M.: Rhizosphere humic acid interacts with root cell walls to reduce hydraulic conductivity and plant development, Plant Soil, 336, 313–322, https://doi.org/10.1007/s11104-010-0483-2, 2010.

Avena, M. J. and Wilkinson, K. J.: Disaggregation kinetics of a peat humic acid: Mechanism and pH effects, Environ Sci Technol, 36, 5100–5105, https://doi.org/10.1021/es025582u, 2002.

Benes, P.: Radiotracer study of thorium complexation with humic acid at pH 2-11 using free-liquid electrophoresis, Radiochim Acta, 97, 273–281, https://doi.org/10.1524/ract.2009.1611, 2009.

Boguta, P., D'Orazio, V., Sokołowska, Z., and Senesi, N.: Effects of selected chemical and physicochemical properties of humic acids from peat soils on their interaction mechanisms with copper ions at various pH, J Geochem Explor, 168, 119–126, https://doi.org/10.1016/j.gexplo.2016.06.004, 2016.

Boguta, P., D'Orazio, V., Senesi, N., Sokołowska, Z., and Szewczuk-Karpisz, K.: Insight into the interaction mechanism of iron ions with soil humic acids. The effect of the pH and chemical properties of humic acids, J Environ Manage, 245, 367–374, https://doi.org/10.1016/j.jenvman.2019.05.098, 2019.

Bond-Lamberty, B. and Thomson, A.: Temperature-associated increases in the global soil respiration record, Nature, 464, 579–582, https://doi.org/10.1038/nature08930, 2010.

Brady, C. N. and Weil, R. R.: The Nature and Properties of Soils, 14th Edition [Hardcover], 980 pp., 2008.

Bronick, C. J. and Lal, R.: Soil structure and management: A review, Geoderma, 124, 3–22, https://doi.org/10.1016/j.geoderma.2004.03.005, 2005.

Bryan, N. D., Abrahamsen, L., Evans, N., Warwick, P., Buckau, G., Weng, L., and Van Riemsdijk, W. H.: The effects of humic substances on the transport of radionuclides: Recent improvements in the prediction of behaviour and the understanding of mechanisms, Applied Geochemistry, 27, 378–389, https://doi.org/10.1016/j.apgeochem.2011.09.008, 2012.

Canellas, L. P. and Olivares, F. L.: Physiological responses to humic substances as plant growth promoter, Chemical and Biological Technologies in Agriculture, 1, 1–11, https://doi.org/10.1186/2196-5641-1-3, 2014.

Chassapis, K., Roulia, M., and Nika, G.: Fe(III)-humate complexes from Megalopolis peaty lignite: A novel eco-friendly fertilizer, Fuel, 89, 1480–1484, https://doi.org/10.1016/j.fuel.2009.10.005, 2010.

Chen, C., Hall, S. J., Coward, E., and Thompson, A.: Iron-mediated organic matter decomposition in humid soils can counteract protection, Nat Commun, 11, 1–13, https://doi.org/10.1038/s41467-020-16071-5, 2020.

Chen, H., Abdulla, H. A. N., Sanders, R. L., Myneni, S. C. B., Mopper, K., and Hatcher, P. G.: Production of Black Carbon-like and Aliphatic Molecules from Terrestrial Dissolved Organic Matter in the Presence of Sunlight and Iron, Environ Sci Technol Lett, 1, 399–404, https://doi.org/10.1021/ez5002598, 2014.

Chou, P. I., Ng, D. Q., Li, I. C., and Lin, Y. P.: Effects of dissolved oxygen, pH, salinity and humic acid on the release of metal ions from PbS, CuS and ZnS during a simulated storm event, Science of the Total Environment, 624, 1401–1410, https://doi.org/10.1016/j.scitotenv.2017.12.221, 2018.

Christl, I., Metzger, A., Heidmann, I., and Kretzschmar, R.: Effect of humic and fulvic acid concentrations and ionic strength on copper and lead binding, Environ Sci Technol, 39, 5319–5326, https://doi.org/10.1021/es050018f, 2005.

Ciceri, D. and Allanore, A.: Microfluidic leaching of soil minerals: Release of K+ from K feldspar, PLoS One, 10, 1–10, https://doi.org/10.1371/journal.pone.0139979, 2015.

Coble, P. G., Green, S. A., Blough, N. V., and Gagosian, R. B.: Characterization of dissolved organic matter in the Black Sea by fluorescence spectroscopy, Nature, 348, 432–435, 1990.

Coble, P. G.: Characterization of marine and terrestrial DOM in sea water using excitation-emission matrix spectroscopy, Mar. Chem., 52, 325–346, 1996.

Cory, R. M. and McKnight, D. M.: Fluorescence spectroscopy reveals ubiquitous presence of oxidized and reduced quinones in dissolved organic matter, Environ Sci Technol, 39, 8142–8149,

https://doi.org/10.1021/ES0506962/SUPPL_FILE/ES0506962SI20050808_031842.PDF, 2005.

Crowther, T. W., Todd-Brown, K. E. O., Rowe, C. W., Wieder, W. R., Carey, J. C., MacHmuller, M. B., Snoek, B. L., Fang, S., Zhou, G., Allison, S. D., Blair, J. M., Bridgham, S. D., Burton, A. J., Carrillo, Y., Reich, P. B., Clark, J. S., Classen, A. T., Dijkstra, F. A., Elberling, B., Emmett, B. A., Estiarte, M., Frey, S. D., Guo, J., Harte, J., Jiang, L., Johnson, B. R., Kroël-Dulay, G., Larsen, K. S., Laudon, H., Lavallee, J. M., Luo, Y., Lupascu, M., Ma, L. N., Marhan, S., Michelsen, A., Mohan, J., Niu, S., Pendall, E., Peñuelas, J., Pfeifer-Meister, L., Poll, C., Reinsch, S., Reynolds, L. L., Schmidt, I. K., Sistla, S., Sokol, N. W., Templer, P. H., Treseder, K. K., Welker, J. M., and Bradford, M. A.: Quantifying global soil carbon losses in response to warming, Nature, 540, 104–108, https://doi.org/10.1038/nature20150, 2016.

Curtin, D., Beare, M. H., Chantigny, M. H., and Greenfield, L. G.: Controls on the Extractability of Soil Organic Matter in Water over the 20 to 80°C Temperature Range, Soil Science Society of America Journal, 75, 1423–1430, https://doi.org/10.2136/sssaj2010.0401, 2011.

Davidson, E. A. and Janssens, I. A.: Temperature sensitivity of soil carbon decomposition and feedbacks to climate change, Nature, 440, 165–173, https://doi.org/10.1038/nature04514, 2006.

De la Rosa, J. M., Faria, S. R., Varela, M. E., Knicker, H., González-Vila, F. J., González-Pérez, J. A., and Keizer, J.: Characterization of wildfire effects on soil organic matter using analytical pyrolysis, Geoderma, 191, 24–30, https://doi.org/10.1016/J.GEODERMA.2012.01.032, 2012.

Demyan, M. S. et al.: Use of specific peaks obtained by diffuse reflectance Fourier transform mid-infrared spectroscopy to study the composition of organic matter in a Haplic Chernozem, European Journal of Soil Science, 63, 189–199, 2012.

Drake, T. W., Van Oost, K., Barthel, M., Bauters, M., Hoyt, A. M., Podgorski, D. C., Six, J., Boeckx, P., Trumbore, S. E., Cizungu Ntaboba, L., and Spencer, R. G. M.: Mobilization of aged and biolabile soil carbon by tropical deforestation, Nat Geosci, 12, 541–546, https://doi.org/10.1038/s41561-019-0384-9, 2019.

Dynarski, K. A., Bossio, D. A., and Scow, K. M.: Dynamic Stability of Soil Carbon: Reassessing the "Permanence" of Soil Carbon Sequestration, Front Environ Sci, 8, 514701, https://doi.org/10.3389/FENVS.2020.514701/BIBTEX, 2020.

Ellerbrock, R. H., Gerke, H. H., and Deumlich, D.: Soil organic matter composition along a slope in an erosion-affected arable landscape in North East Germany, Soil Tillage Res, 156, 209–218, https://doi.org/10.1016/J.STILL.2015.08.014, 2016.

Fang, C., Smith, P., Moncrieff, J. B., and Smith, J. U.: Similar response of labile and resistant soil organic matter pools to changes in temperature, Nature, 433, 57–59, https://doi.org/10.1038/nature03138, 2005.

Fulda, B., Voegelin, A., Maurer, F., Christl, I., and Kretzschmar, R.: Copper Redox Transformation and Complexation by Reduced and Oxidized Soil Humic Acid. 1. X-ray Absorption Spectroscopy Study, Environ Sci Technol, 47, 10903–10911, 2013.

Gabor, R. S., Burns, M. A., Lee, R. H., Elg, J. B., Kemper, C. J., Barnard, H. R., and McKnight, D. M.: Influence of leaching solution and catchment location on the fluorescence of water-soluble organic matter, Environ Sci Technol, 49, 4425–4432, https://doi.org/10.1021/es504881t, 2015.

Gao, J., Lv, J., Wu, H., Dai, Y., and Nasir, M.: Impacts of wheat straw addition on dissolved organic matter characteristics in cadmium-contaminated soils: Insights from fluorescence spectroscopy and environmental implications, Chemosphere, 193, 1027–1035, https://doi.org/10.1016/j.chemosphere.2017.11.112, 2018a.

Gao, L., Zhou, Z., Reyes, A. V., and Guo, L.: Yields and Characterization of Dissolved Organic Matter From Different Aged Soils in Northern Alaska, J Geophys Res Biogeosci, 123, 2035–2052, https://doi.org/10.1029/2018JG004408, 2018b.

Gao, X., Zhang, J., Mostofa, K. M. G., Zheng, W., Liu, C. Q., Senesi, N., Senesi, G. S., Vione, D., Yuan, J, Liu, Y., Mohinuzzaman, M., Li, L., and Li, S. L.: Sulfur-mediated transformation, export and mineral complexation of organic and inorganic C, N, P and Si in dryland soils. Scientific Reporrts. under review (revising based on positive review comments), 2025.

Garcia-Mina, J. M.: Stability, solubility and maximum metal binding capacity in metal-humic complexes involving humic substances extracted from peat and organic compost, Org Geochem, 37, 1960–1972, https://doi.org/10.1016/j.orggeochem.2006.07.027, 2006.

Gilbert, B., Lu, G., and Kim, C. S.: Stable cluster formation in aqueous suspensions of iron oxyhydroxide nanoparticles, J. Colloid Interface Sci, 313, 152–159, 2007.

Green, J. K., Seneviratne, S. I., Berg, A. M. et al.: Large influence of soil moisture on long-term terrestrial carbon uptake, Nature, 565, 476–479, https://doi.org/10.1038/s41586-018-0848-x, 2019.

Haitzer, M., Aiken, G. R., and Ryan, J. N.: Binding of mercury(II) to dissolved organic matter: The role of the mercury-

to-DOM concentration ratio, Environ Sci Technol, 36, 3564–3570, https://doi.org/10.1021/es025699i, 2002.
Haitzer, M., Aiken, G. R., and Ryan, J. N.: Binding of mercury(II) to aquatic humic substances: Influence of pH and source of humic substances, Environ Sci Technol, 37, 2436–2441, https://doi.org/10.1021/es026291o, 2003.
Harden, J. W., Hugelius, G., Ahlström, A., Blankinship, J. C., Bond-Lamberty, B., Lawrence, C. R., Loisel, J., Malhotra, A., Jackson, R. B., Ogle, S., Phillips, C., Ryals, R., Todd-Brown, K., Vargas, R., Vergara, S. E., Cotrufo, M. F., Keiluweit, M., Heckman, K. A., Crow, S. E., Silver, W. L., DeLonge, M., and Nave, L. E.: Networking our science to characterize the state, vulnerabilities, and management opportunities of soil organic matter, Glob Chang Biol, 24, e705–e718, https://doi.org/10.1111/gcb.13896, 2018.
Heitmann, T., Goldhammer, T., Beer, J., and Blodau, C.: Electron transfer of dissolved organic matter and its potential significance for anaerobic respiration in a northern bog, Glob Chang Biol, 13, 1771–1785, https://doi.org/10.1111/j.1365-2486.2007.01382.x, 2007.
Helms, J. R., Mao, J., Schmidt-Rohr, K., Abdulla, H., and Mopper, K.: Photochemical flocculation of terrestrial dissolved organic matter and iron, Geochim Cosmochim Acta, 121, 398–413, https://doi.org/10.1016/j.gca.2013.07.025, 2013.
Heckman, D. S. et al.: Molecular Evidence for the Early Colonization of Land by Fungi and Plants. Science 293, 1129, 2001.
Hemingway, J. D., Rothman, D. H., Grant, K. E., Rosengard, S. Z., Eglinton, T. I., Derry, L. A., and Galy, V. v.: Mineral protection regulates long-term global preservation of natural organic carbon, Nature 2019 570:7760, 570, 228–231, https://doi.org/10.1038/s41586-019-1280-6, 2019.
Hernández, D., Plaza, C., Senesi, N., and Polo, A.: Detection of Copper(II) and zinc(II) binding to humic acids from pig slurry and amended soils by fluorescence spectroscopy, Environmental Pollution, 143, 212–220, https://doi.org/10.1016/j.envpol.2005.11.038, 2006.
Huang, W. and Hall, S. J.: Elevated moisture stimulates carbon loss from mineral soils by releasing protected organic matter, Nat Commun, 8, https://doi.org/10.1038/s41467-017-01998-z, 2017.
Jiang, T., Skyllberg, U., Wei, S., Wang, D., Lu, S., Jiang, Z., and Flanagan, D. C.: Modeling of the structure-specific kinetics of abiotic, dark reduction of Hg(II) complexed by O/N and S functional groups in humic acids while accounting for time-dependent structural rearrangement, Geochim Cosmochim Acta, 154, 151–167, https://doi.org/10.1016/j.gca.2015.01.011, 2015.
Jones, K. D. and Tiller, C. L.: Effect of solution chemistry on the extent of binding of phenanthrene by a soil humic acid: A comparison of dissolved and clay bound humic, Environ Sci Technol, 33, 580–587, https://doi.org/10.1021/es9803207, 1999.
Jovanovic´, U. D., Jovanovic´1, J., Markovic´, M. M., Markovic´, M., Cupac´, S. B., Cupac´, C., Tomic´, Z. P., and Tomic´, T.: Soil humic acid aggregation by dynamic light scattering and laser Doppler electrophoresis, Journal of Plant Nutrition and Soil Science, 176, 674–679, https://doi.org/10.1002/JPLN.201200346, 2013.
Kallenbach, C., Frey, S., and Grandy, A.: Direct evidence for microbial-derived soil organic matter formation and its ecophysiological controls, Nature Communications 7, 13630, https://doi.org/10.1038/ncomms13630, 2016.
Karadirek, Ş., Kanmaz, N., Balta, Z., Demirçivi, P., Üzer, A., Hizal, J., and Apak, R.: Determination of total antioxidant capacity of humic acids using CUPRAC, Folin–Ciocalteu, noble metal nanoparticle- and solid–liquid extraction-based methods, Talanta, 153, 120–129, https://doi.org/10.1016/J.TALANTA.2016.03.006, 2016.
Kirsten, M., Mikutta, R., Vogel, C., Thompson, A., Mueller, C. W., Kimaro, D. N., Bergsma, H. L. T., Feger, K. H., and Kalbitz, K.: Iron oxides and aluminous clays selectively control soil carbon storage and stability in the humid tropics, Scientific Reports 2021 11:1, 11, 1–12, https://doi.org/10.1038/s41598-021-84777-7, 2021.
Klapper, L., McKnight, D. M., Fulton, J. R., Blunt-Harris, E. L., Nevin, K. P., Lovley, D. R., and Hatcher, P. G.: Fulvic acid oxidation state detection using fluorescence spectroscopy, Environ Sci Technol, 36, 3170–3175, https://doi.org/10.1021/ES0109702/ASSET/IMAGES/LARGE/ES0109702F00004.JPEG, 2002.
Kleber, M., Sollins, P., and Sutton, R.: A conceptual model of organo-mineral interactions in soils: Self-assembly of organic molecular fragments into zonal structures on mineral surfaces, Biogeochemistry, 85, 9–24, https://doi.org/10.1007/s10533-007-9103-5, 2007.
Kleber, M., Bourg, I. C., Coward, E. K., Hansel, C. M., Myneni, S. C. B., and Nunan, N.: Dynamic interactions at the mineral–organic matter interface, Nature Reviews Earth & Environment 2021 2:6, 2, 402–421, https://doi.org/10.1038/s43017-021-00162-y, 2021.
Klüpfel, L., Piepenbrock, A., Kappler, A., and Sander, M.: Humic substances as fully regenerable electron acceptors in recurrently anoxic environments, Nat Geosci, 7, 195–200, https://doi.org/10.1038/ngeo2084, 2014.
Kothawala, D. N., Murphy, K. R., Stedmon, C. A., Weyhenmeyer, G. A., and Tranvik, L. J.: Inner filter correction of

dissolved organic matter fluorescence, Limnol Oceanogr Methods, 11, 616–630, https://doi.org/10.4319/lom.2013.11.616, 2013.

Kunlanit, B., Vityakon, P., Puttaso, A., Cadisch, G., and Rasche, F.: Mechanisms controlling soil organic carbon composition pertaining to microbial decomposition of biochemically contrasting organic residues: Evidence from midDRIFTS peak area analysis, Soil Biology and Biochemistry 76, 100–108, 2014.

Lalonde, K., Mucci, A., Ouellet, A., and Gélinas, Y.: Preservation of organic matter in sediments promoted by iron, Nature 2012 483:7388, 483, 198–200, https://doi.org/10.1038/nature10855, 2012.

Lange, O. L., Belnap, J., and Reichenberger, H.: Photosynthesis of the cyanobacterial soil-crust lichen Collema tenax from arid lands in southern Utah, USA: Role of water content on light and temperature responses of CO_2 exchange. Functional Ecology, 12, 195-202, 1998.

Leenheer, J. A., Wershaw, R. L., and Reddy, M. M.: Strong-Acid, Cariioxyl-Group Structures in Fulvic Acid from the Suwannee River, Georgia. 2. Major Structures, Environ Sci Technol, 29, 399–405, https://doi.org/10.1021/es00002a016, 1995.

Lehmann, J. and Kleber, M.: The contentious nature of soil organic matter, Nature 2015 528:7580, 528, 60–68, https://doi.org/10.1038/nature16069, 2015.

Levicán, G. et al.: Comparative genomic analysis of carbon and nitrogen assimilation mechanisms in three indigenous bioleaching bacteria: predictions and validations, BMC Genomics, 2008, 9, 581, 2008.

Li, H. and Vaughan, J. C.: Switchable Fluorophores for Single-Molecule Localization Microscopy, Chem Rev, 118, 9412–9454, https://doi.org/10.1021/acs.chemrev.7b00767, 2018.

Li, Q., Chen, X., Veroustraete, F., Bao, A. M., Liu, T., and Wang, J. L.: Validation of soil moisture retrieval in arid and semi-arid areas, Shuikexue Jinzhan/Advances in Water Science, 21, 201–207, 2010.

Lippold, H., Evans, N. D. M., Warwick, P., and Kupsch, H.: Competitive effect of iron(III) on metal complexation by humic substances: Characterisation of ageing processes, Chemosphere, 67, 1050–1056, https://doi.org/10.1016/j.chemosphere.2006.10.045, 2007.

Liu, J., Mu, Y., Geng, C., Yu, Y., He, H., and Zhang, Y.: Uptake and conversion of carbonyl sulfide in a lawn soil, Atmos Environ, 41, 5697–5706, https://doi.org/10.1016/j.atmosenv.2007.02.039, 2007.

Lundström, U. S., Van Breemen, N., and Bain, D.: The podzolization process. A review, https://doi.org/10.1016/S0016-7061(99)00036-1, 1 February 2000.

Lützow, M. V., Kögel-Knabner, I., Ekschmitt, K., Matzner, E., Guggenberger, G., Marschner, B., and Flessa, H.: Stabilization of organic matter in temperate soils: Mechanisms and their relevance under different soil conditions - A review, Eur J Soil Sci, 57, 426–445, https://doi.org/10.1111/j.1365-2389.2006.00809.x, 2006.

Ma, H. et al.: Rice Planting Increases Biological Nitrogen Fixation in Acidic Soil and the Influence of Light and Flood Layer Thickness, Journal of Soil Science and Plant Nutrition, 21, 341–348, 2021.

Makiel, M., Skiba, M., Kisiel, M., Maj-Szeliga, K., Błachowski, A., Szymański, W., and Salata, D.: Formation of iron oxyhydroxides as a result of glauconite weathering in soils of temperate climate, Geoderma, 416, 115780, https://doi.org/10.1016/J.GEODERMA.2022.115780, 2022.

Malik, A. A., Puissant, J., Buckeridge, K. M., Goodall, T., Jehmlich, N., Chowdhury, S., et al.: Land use driven change in soil pH affects microbial carbon cycling processes, Nature Communications 9, 3591, https://doi.org/10.1038/s41467-018-05980-1, 2018.

Marschner, B., Brodowski, S., Dreves, A., Gleixner, G., Gude, A., Grootes, P. M., Hamer, U., Heim, A., Jandl, G., Ji, R., Kaiser, K., Kalbitz, K., Kramer, C., Leinweber, P., Rethemeyer, J., Schäffer, A., Schmidt, M. W. I., Schwark, L., and Wiesenberg, G. L. B.: How relevant is recalcitrance for the stabilization of organic matter in soils?, Journal of Plant Nutrition and Soil Science, 171, 91–110, https://doi.org/10.1002/jpln.200700049, 2008.

Masaki, Y., Ozawa, R., Kageyama, K., and Katayama, Y.: Degradation and emission of carbonyl sulfide, an atmospheric trace gas, by fungi isolated from forest soil, FEMS Microbiol Lett, 363, 3–5, https://doi.org/10.1093/femsle/fnw197, 2016.

Min, K., Lehmeier, C. A., Ballantyne, F., Tatarko, A., and Billings, S. A.: Differential effects of pH on temperature sensitivity of organic carbon and nitrogen decay, Soil Biol Biochem, 76, 193–200, https://doi.org/10.1016/J.SOILBIO.2014.05.021, 2014.

Mohinuzzaman, M., Yuan, J., Yang, X., Senesi, N., Li, S. L., Ellam, R. M., Mostofa, K. M. G., and Liu, C. Q.: Insights into solubility of soil humic substances and their fluorescence characterisation in three characteristic soils, Science of the Total Environment, 720, 1–38, https://doi.org/10.1016/j.scitotenv.2020.137395, 2020.

Mora, V., Baigorri, R., Bacaicoa, E., Zamarreño, A. M., and García-Mina, J. M.: The humic acid-induced changes in the root concentration of nitric oxide, IAA and ethylene do not explain the changes in root architecture caused by humic acid in cucumber, Environ Exp Bot, 76, 24–32, https://doi.org/10.1016/j.envexpbot.2011.10.001,

2012.
Mostofa, K. M. G., Yoshioka, T., Mottaleb, M. A., Vione, D.: Photobiogeochemistry of Organic Matter: Principles and Practices in Water Environments. Springer, Berlin, Germany, 2013.
Mostofa, K. M. G., Li, W., Wu, F., Liu, C. Q., Liao, H., Zeng, L., and Xiao, M.: Environmental characteristics and changes of sediment pore water dissolved organic matter in four Chinese lakes, Environmental Science and Pollution Research, 25, 2783–2804, https://doi.org/10.1007/s11356-017-0545-6, 2018.
Mostofa, K. M. G., Jie, Y., Sakugawa, H., and Liu, C. Q.: Equal Treatment of Different EEM Data on PARAFAC Modeling Produces Artifact Fluorescent Components That Have Misleading Biogeochemical Consequences, Environ Sci Technol, 53, 561–563, https://doi.org/10.1021/acs.est.8b06647, 2019.
Noy, A., Vezenov, D., and Lieber, C.: Chemical force microscopy Cited by me, Annual Review of Materials Science, 381–421, 1997.
Nurmi, J. T. and Tratnyek, P. G.: Electrochemical properties of natural organic matter (NOM), fractions of NOM, and model biogeochemical electron shuttles, Environ Sci Technol, 36, 617–624, https://doi.org/10.1021/ES0110731/SUPPL_FILE/ES0110731_S.PDF, 2002.
Paul, E. A.: The nature and dynamics of soil organic matter: Plant inputs, microbial transformations, and organic matter stabilization, Soil Biology and Biochemistry, 98, 109-126, 2016.
Peinemann, N., Guggenberger, G., and Zech, W.: Soil organic matter and its lignin component in surface horizons of salt-affected soils of the Argentinian Pampa, Catena (Amst), 60, 113–128, https://doi.org/10.1016/J.CATENA.2004.11.008, 2005.
Pietikäinen, J., Pettersson, M., and Bååth, E.: Comparison of temperature effects on soil respiration and bacterial and fungal growth rates, FEMS Microbiol Ecol, 52, 49–58, https://doi.org/10.1016/j.femsec.2004.10.002, 2005.
Ritchie, J. D. and Michael Perdue, E.: Proton-binding study of standard and reference fulvic acids, humic acids, and natural organic matter, Geochim Cosmochim Acta, 67, 85–96, https://doi.org/10.1016/S0016-7037(02)01044-X, 2003.
Robarge, W. P.: Precipitation/dissolution reactions in soils, in: Soil Physical Chemistry, Second Edition, edited by: Sparks, D. L., CRC Press, Boca Raton, 193–238, https://doi.org/10.1201/9780203739280, 2018.
Ronchi, B., Clymans, W., Barão, A. L. P., Vandevenne, F., Struyf, E., Batelaan, O., Dassargues, A., and Govers, G.: Transport of Dissolved Si from Soil to River: A Conceptual Mechanistic Model, Silicon, 5, 115–133, https://doi.org/10.1007/s12633-012-9138-7, 2013.
Rousk, J., Brookes, P. C., and Bååth, E.: Contrasting soil pH effects on fungal and bacterial growth suggest functional redundancy in carbon mineralization, Appl Environ Microbiol, 75, 1589–1596, https://doi.org/10.1128/AEM.02775-08, 2009.
Saito, T., Nagasaki, S., and Tanaka, S.: Molecular fluorescence spectroscopy and mixture analysis for the evaluation of the complexation between humic acid and UO22+, Radiochim Acta, 90, 545–548, https://doi.org/10.1524/ract.2002.90.9-11_2002.545, 2002.
dos Santos, J. V., Fregolente, L. G., Mounier, S., Hajjoul, H., Ferreira, O. P., Moreira, A. B., and Bisinoti, M. C.: Fulvic acids from Amazonian anthropogenic soils: Insight into the molecular composition and copper binding properties using fluorescence techniques, Ecotoxicol Environ Saf, 205, https://doi.org/10.1016/j.ecoenv.2020.111173, 2020.
Schmidt, W., Santi, S., Pinton, R., and Varanini, Z.: Water-extractable humic substances alter root development and epidermal cell pattern in Arabidopsis, Plant Soil, 300, 259–267, https://doi.org/10.1007/s11104-007-9411-5, 2007.
Senesi, N.: Molecular and quantitative aspects of the chemistry of fulvic acid and its interactions with metal ions and organic chemicals. Part II. The fluorescence spectroscopy approach, Anal Chim Acta, 232, 77–106, https://doi.org/10.1016/S0003-2670(00)81226-X, 1990a.
Senesi, N.: Molecular and quantitative aspects of the chemistry of fulvic acid and its interactions with metal ions and organic chemicals. Part I. The electron spin resonance approach, Anal Chim Acta, 232, 51–75, https://doi.org/10.1016/S0003-2670(00)81225-8, 1990b.
Senesi, N. and Loffredo, E.: The Chemistry of Soil Organic Matter in Soil Physical Chemistry, 2nd ed, 1999.
Senesi, N. and Plaza, C.: Role of humification processes in recycling organic wastes of various nature and sources as soil amendments, Clean (Weinh), 35, 26–41, https://doi.org/10.1002/clen.200600018, 2007.
Senesi, N., D'Orazio, V., and Ricca, G.: Humic acids in the first generation of EUROSOILS, Geoderma, 116, 325–344, https://doi.org/10.1016/S0016-7061(03)00107-1, 2003.
Shammi, M., Pan, X., Mostofa, K. M. G., Zhang, D., Liu, C. Q.: Photo-flocculation of algal biofilm extracellular polymeric substances and its transformation into transparent exopolymer particles. Chemical and spectroscopic evidences. Scientific Reports 7, 9074, 2017.

Singh, R. P. et al.: Isolation and characterization of exopolysaccharides from seaweed associated bacteria Bacillus licheniformis. Carbohydrate Polymers, 84, 1019–1026, 2011.
Six, J., Conant, R. T., Paul, E. A., and Paustian, K.: 2002 Six Stabilizatio nmechanisms of SOM implications for C saturation of soils.pdf, Plant Soil, 241, 155–176, 2002.
Sollins, P., Homann, P., and Caldwell, B. A.: Stabilization and destabilization of soil organic matter: mechanisms and controls Phillip, Geoderma, 74, 65–105, 1996.
Song, Z., McGrouther, K., and Wang, H.: Occurrence, turnover and carbon sequestration potential of phytoliths in terrestrial ecosystems, Earth Sci Rev, 158, 19–30, https://doi.org/10.1016/j.earscirev.2016.04.007, 2016.
Soti, P. G., Jayachandran K., Koptur, S., and Volin J.C.: Effect of soil pH on growth, nutrient uptake, and mycorrhizal colonization in exotic invasive Lygodium microphyllum, Plant Ecology, 216, 989-998, 2015.
Spence, A. and Kelleher, B. P.: Photodegradation of major soil microbial biomolecules is comparable to biodegradation: Insights from infrared and diffusion editing NMR spectroscopies, J Mol Struct, 1107, 7–13, https://doi.org/10.1016/j.molstruc.2015.11.025, 2016.
Stedmon, C. A., Markager, S., and Bro, R.: Tracing dissolved organic matter in aquatic environments using a new approach to fluorescence spectroscopy, Mar Chem, 82, 239–254, https://doi.org/10.1016/S0304-4203(03)00072-0, 2003.
Steinmuller, H. E. and Chambers, L. G.: Characterization of coastal wetland soil organic matter: Implications for wetland submergence, Science of The Total Environment, 677, 648–659, https://doi.org/10.1016/J.SCITOTENV.2019.04.405, 2019.
Stolpe, B., Guo, L., and Shiller, A. M.: Binding and transport of rare earth elements by organic and iron-rich nanocolloids in alaskan rivers, as revealed by field-flow fractionation and ICP-MS, Geochim Cosmochim Acta, 106, 446–462, https://doi.org/10.1016/j.gca.2012.12.033, 2013.
Szulczewski, M. D., Helmke, P. A., and Bleam, W. F.: XANES spectroscopy studies of Cr(VI) reduction by thiols in organosulfur compounds and humic substances, Environ Sci Technol, 35, 1134–1141, https://doi.org/10.1021/es001301b, 2001.
Tadini, A. M., Nicolodelli, G., Senesi, G. S., Ishida, D. A., Montes, C. R., Lucas, Y., Mounier, S., Guimarães, F. E. G., and Milori, D. M. B. P.: Soil organic matter in podzol horizons of the Amazon region: Humification, recalcitrance, and dating, Science of the Total Environment, 613–614, 160–167, https://doi.org/10.1016/j.scitotenv.2017.09.068, 2018.
Tadini, A. M., Mounier, S., and Milori, D. M. B. P.: Modeling the quenching of fluorescence from organic matter in Amazonian soils, Science of the Total Environment, 698, 134067, https://doi.org/10.1016/j.scitotenv.2019.134067, 2020.
Tremblay, L., Kohl, S. D., Rice, J. A., and Gagné, J. P.: Effects of temperature, salinity, and dissolved humic substances on the sorption of polycyclic aromatic hydrocarbons to estuarine particles, Mar Chem, 96, 21–34, https://doi.org/10.1016/j.marchem.2004.10.004, 2005.
Trevisan, S., Pizzeghello, D., Ruperti, B., Francioso, O., Sassi, A., Palme, K., Quaggiotti, S., and Nardi, S.: Humic substances induce lateral root formation and expression of the early auxin-responsive IAA19 gene and DR5 synthetic element in Arabidopsis, Plant Biol, 12, 604–614, https://doi.org/10.1111/j.1438-8677.2009.00248.x, 2010.
Underwood, T. R. et al.: Mineral-associated organic matter is heterogeneous and structured by hydrophobic, charged, and polar interactions, PNAS 121, e2413216121, https://doi.org/10.1073/pnas.2413216121, 2024.
Varghese, E.M., et al.: Rice in acid sulphate soils: Role of microbial interactions in crop and soil health management. Applied Soil Ecology, 196, 105309, 2024.
Vezenov, D. V., Noy, A., Rozsnyai, L. F., and Lieber, C. M.: Force titrations and ionization state sensitive imaging of functional groups in aqueous solutions by chemical force microscopy, J Am Chem Soc, 119, 2006–2015, https://doi.org/10.1021/ja963375m, 1997.
Vezenov, D. V., Noy, A., and Ashby, P.: Chemical force microscopy: Probing chemical origin of interfacial forces and adhesion, J Adhes Sci Technol, 19, 313–364, https://doi.org/10.1163/1568561054352702, 2005.
Vidali, R., Remoundaki, E., and Tsezos, M.: Humic acids copper binding following their photochemical alteration by simulated solar light, Aquat Geochem, 16, 207–218, https://doi.org/10.1007/s10498-009-9080-5, 2010.
Vogel, C., Mueller, C. W., Höschen, C., Buegger, F., Heister, K., Schulz, S., Schloter, M., and Kögel-Knabner, I.: Submicron structures provide preferential spots for carbon and nitrogen sequestration in soils, Nat Commun, 5, 1–7, https://doi.org/10.1038/ncomms3947, 2014.
Wang, C., Cheng, T., Zhang, D., and Pan, X.: Electrochemical properties of humic acid and its novel applications: A tip of the iceberg, Science of The Total Environment, 863, 160755, https://doi.org/10.1016/J.SCITOTENV.2022.160755, 2023.

Wang, L. F., Wang, L. L., Ye, X. D., Li, W. W., Ren, X. M., Sheng, G. P., Yu, H. Q., and Wang, X. K.: Coagulation kinetics of humic aggregates in mono- and Di-valent electrolyte solutions, Environ Sci Technol, 47, 5042–5049, https://doi.org/10.1021/es304993j, 2013.

Ward, N. D., Keil, R. G., Medeiros, P. M., Brito, D. C., Cunha, A. C., Dittmar, T., Yager, P. L., Krusche, A. V., and Richey, J. E.: Degradation of terrestrially derived macromolecules in the Amazon River, Nat Geosci, 6, 530–533, https://doi.org/10.1038/NGEO1817, 2013.

Whalen, E. D., et al.: Microbial trait multifunctionality drives soil organic matter formation potential. Nature Communications, 15, 10209, 2024.

Whelan, M. E. and Rhew, R. C.: Carbonyl sulfide produced by abiotic thermal and photodegradation of soil organic matter from wheat field substrate, J Geophys Res Biogeosci, 120, 54–62, https://doi.org/10.1002/2014JG002661, 2015.

WRB, I., Schád, P., van Huyssteen, C., and Micheli, E.: World Reference Base for Soil Resources 2014, update 2015, 2015.

Wu, F., Cai, Y., Evans, D., and Dillon, P.: Complexation between Hg (II) and Dissolved Organic Matter in Stream Waters : An Application of Fluorescence Spectroscopy, Biogeochemistry, 71, 339–351, 2004a.

Wu, F., Mills, R. B., Evans, R. D., and Dillon, P. J.: Kinetics of Metal−Fulvic Acid Complexation Using a Stopped-Flow Technique and Three-Dimensional Excitation Emission Fluorescence Spectrophotometer, American Chemical Society, 76, 110–113, 2004b.

Xi, M., Zi, Y., Wang, Q., Wang, S., Cui, G., and Kong, F.: Assessment of the content, structure, and source of soil dissolved organic matter in the coastal wetlands of Jiaozhou Bay, China, Physics and Chemistry of the Earth, 103, 35–44, https://doi.org/10.1016/j.pce.2017.03.004, 2018.

Xie, H., Zafiriou, O. C., Cai, W. J., Zepp, R. G., and Wang, Y.: Photooxidation and its effects on the carboxyl content of dissolved organic matter in two coastal rivers in the southeastern United States, Environ Sci Technol, 38, 4113–4119, https://doi.org/10.1021/es035407t, 2004.

Yang, X., Yuan, J., Yue, F. J., Li, S. L., Wang, B., Mohinuzzaman, M., Liu, Y., Senesi, N., Lao, X., Li, L., Liu, C. Q., Ellam, R. M., Vione, D., and Mostofa, K. M. G.: New insights into mechanisms of sunlight- and dark-mediated high-temperature accelerated diurnal production-degradation of fluorescent DOM in lake waters, Science of the Total Environment, 760, 143377, https://doi.org/10.1016/j.scitotenv.2020.143377, 2021.

Yang, Z., Kappler, A., and Jiang, J.: Reducing capacities and distribution of redox-active functional groups in low molecular weight fractions of humic acids, Environ Sci Technol, 50, 12105–12113, https://doi.org/10.1021/ACS.EST.6B02645/ASSET/IMAGES/LARGE/ES-2016-02645B_0007.JPEG, 2016.

Yang, X., Gao, X., Mostofa, K. M. G., Zheng, W., Senesi, N., Senesi, G. S., Vione, D., Yuan, J., Li, S. L., Li, L., Liu, C. Q.: Mineral states and sequestration processes involving soil biogenic components in various soils and desert sands of Inner Mongolia, Scientific Reports 14, 28530, https://doi.org/10.1038/s41598-024-80004-1, 2024.

Yu, G. H., Chi, Z. L., Kappler, A., Sun, F. S., Liu, C. Q., Teng, H. H., and Gadd, G. M.: Fungal Nanophase Particles Catalyze Iron Transformation for Oxidative Stress Removal and Iron Acquisition, Current Biology, 30, 2943-2950.e4, https://doi.org/10.1016/j.cub.2020.05.058, 2020.

Zhang, D., Pan, X., Mostofa, K. M. G., Chen, X., Mu, G., Wu, F., Liu, J., Song, W., Yang, J., Liu, Y., and Fu, Q.: Complexation between Hg(II) and biofilm extracellular polymeric substances: An application of fluorescence spectroscopy, J Hazard Mater, 175, 359–365, https://doi.org/10.1016/j.jhazmat.2009.10.011, 2010.

Zhang, J., Mostofa, K. M. G., Yang, X., Mohinuzzaman, M., Liu, C. Q., Senesi, N., Senesi, G. S., Sparks, D. L., Teng, H. H., Li, L., Yuan, J., and Li, S. L.: Isolation of dissolved organic matter from aqueous solution by precipitation with FeCl3: mechanisms and significance in environmental perspectives, Scientific Reports 2023 13:1, 13, 1–15, https://doi.org/10.1038/s41598-023-31831-1, 2023.

Zhu, B. and Ryan, D. K.: Characterizing the interaction between uranyl ion and fulvic acid using regional integration analysis (RIA) and fluorescence quenching, J Environ Radioact, 153, 97–103, https://doi.org/10.1016/j.jenvrad.2015.12.004, 2016.